SERI/STR-211-2542
(DE85002906)
Distribution Category UC-63

Electrochemical Photovoltaic Cells/ Stabilization and Optimization of II-VI Semiconductors

Final Report
15 April 1980-31 July 1982

A Subcontract Report

Dennis Tench
Leslie Warren
Rockwell International

November 1984

Prepared under Subcontract No. XG-0-9276

SERI Technical Monitor: W. Wallace

Solar Energy Research Institute
A Division of Midwest Research Institute

1617 Cole Boulevard
Golden, Colorado 80401

Prepared for the
U.S. Department of Energy
Contract No. DE-AC02-83CH10093

ABSTRACT

This report presents results of research conducted to provide a basis for designing a practical electrochemical solar cell based on the II-VI compound semiconductors. Emphasis is on developing new solvent/redox systems and conducting films that will stabilize the II-VI compounds against photodissolution without seriously degrading the long-term solar response. The use of redox couples in conjunction with protective films seems to be the most promising approach to attaining a practical electrochemical solar cell. Encouraging results have also been obtained for protection of photoanodes with organic films. Electrochemical photocapacitance spectroscopy (EPS) has been a demonstrated as sensitive means of characterizing deep trap levels in semiconductor materials.

TABLE OF CONTENTS

LIST OF FIGURES

LIST OF FIGURES

LIST OF TABLES

LIST OF APPENDICES

1.0 ABSTRACT

The overall goal of this program is to provide the basis for designing a practical electrochemical solar cell based on the II-VI compound semiconductors. Emphasis is on developing new solvent/redox systems and conducting films which will stabilize the II-VI compounds against photodissolution without seriously degrading the long-term solar response.

Based on evaluation of a large number of redox systems, both aqueous and nonaqueous, it appears that improvement in the conversion efficiency for naked semiconductors compared to that offered by the aqueous sulfide/polysulfide system (~ 5%) can only be attained at the expense of photoelectrode stability. Although some photodecomposition occurs, efficiencies in the 10% range have been demonstrated for a few couples, including $Fe(CN)_6^{3-/4}$ and $Fe^{3+/2+}$ in aqueous solutions, and $Fe^{3+/2+}$ and $Cu^{2+/1+}$ in acetonitrile. Use of such redox couples in conjunction with protective films seems to be the most promising approach to attaining a practical electrochemical solar cell.

Encouraging results have been obtained for protection of photoanodes with organic films. Conducting polymer films of polypyrrole photoelectrochemically deposited onto II-VI semiconductors have been shown to protect these electrode materials from photodecomposition while permitting charge transport to the electrolyte, but the polypyrrole itself seems to be unstable and gradually and irreversibly becomes insulating upon repetitive potential cycling in the electrolytes studied. Similar instability was observed with the related polythiophene films. Photoelectrochemical deposition of conducting polyaniline films can be accompanied by semiconductor photodecompositon; the resulting apparently porous films do not afford long-term protection of the electrode surface. Recently, however, films of the electrochromic lutetium diphthalocyanine, which is stable in both acidic and basic media, have been shown to stabilize II-VI photoanodes and permit electron exchange with the electrolyte. In this case, problems associated with electrochemical deposition, i.e., simultaneous photoanode decomposition, are avoided since the film is applied by simple evaporation.

Electrochemically deposited metal oxide/hydroxide films have been formed on conducting surfaces by a new technique. The oxides of manganese, iron, cobalt, nickel, copper and ruthenium have been shown to be conducting in aqueous and nonaqueous electrolytes and are potentially capable of stabilizing narrow-band-gap semiconductors against photodecomposition. A technique for the photoelectrochemical deposition of some of these films on n-CdSe has been developed and initial stabilization studies are encouraging.

One of the key accomplishments during this reporting period was the demonstration that electrochemical photocapacitance spectroscopy (EPS) is a sensitive means of characterizing deep trap levels in semiconductor materials. For horizontal Bridgeman-grown n-GaAs, a hole trap (0.73 eV above the valence band edge), the chromium phototransition (peak at 0.92 eV), and two electron traps (~ 0.8 and 1.09 eV below the conduction band edge) were detected. These levels correlate extremely well with the principal states observed for similar material by solid-state methods. For single crystal n-CdSe, traps were detected at 1.04, 1.21, 1.34 and 1.55 eV below the conduction band edge. Based on a comparison with solid-state literature data, the 1.04 and 1.21 eV traps can be attributed to interface states associated with oxygen adsorption, whereas, the 1.34 and 1.55 eV states are apparently intrinsic to CdSe.

Considerable progress has been made in applying EPS to the characterization of polycrystalline n-CdSe films prepared by evaporation of the elements by the Grumman group. The most significant result is that material prepared at a low substrate temperature contains an appreciable concentration of an electron trap (~ 0.2 eV below the conduction band edge) which is also found in, at most, small concentrations in single crystals and in film material prepared at a high substrate temperature. The implication of these results is that the trap level observed for the low-substrate-temperature material limits the attainable open circuit voltage, and possibly the photocurrent. Similar transitions are observed in polysulfide electrolytes but adsorption of sulfur species on the electrode surface shifts the energies of the transitions and causes the capacitance to drift slowly with time.

2.0 PROJECT DESCRIPTION

To date, the best performance for electrochemical solar cells has been attained with n-type cadmium chalcogenide (CdX, where X = S, Se or Te) [1-15] and n-GaAs [16] electrodes stabilized by chalcogenide/polychalcogenide redox couples (e.g., Se^{2-}/Se_x^{2-}) in aqueous electrolytes. Photogenerated holes, which would otherwise lead to destruction of the semiconductor lattice, are preferentially consumed in the redox reaction. Solar AM2 conversion efficiencies of 7 to 8% for CdX single crystals [10], 6% for thin CdX polycrystalline films [1], and 9% for GaAs single crystals [16] have been reported. Unfortunately, although photodissolution is almost completely suppressed in such systems, the photocurrents deteriorate with time, especially at higher light intensities. In the case of CdX, this has been shown to involve chalcogenide exchange between the electrolyte and the electrode surface, possibly via photo-oxidation followed by reprecipitation [17-20]. Noufi, et al. [1] have demonstrated that conversion efficiencies are higher and degradation is slower for mixed polycrystalline CdS/CdSe electrodes. Chemical modification of n-GaAs electrodes by $RuCl_3$ solutions has also been shown [21] to increase solar conversion efficiencies for single crystals to 12% in Se^{2-}/Se_x^{2-}, although long-term stability has not been established.

These results demonstrate both the promise and the problems associated with stabilization of narrow-band-gap semiconductors for use in electrochemical solar cells. Most studies to date have emphasized cell characterization rather than materials development, so that only the more common semiconductors and a few redox systems have been investigated. In spite of this, decent power conversion efficiencies (6%) for thin polycrystalline films have been demonstrated. To evolve a stable acceptably efficient cell, however, a more systematic approach involving a wider spectrum of materials and more emphasis on materials characterization is needed. The most promising possibilities include both aqueous and nonaqueous redox systems used in conjunction with chemically modified electrode surfaces. Surface chemical modification is particularly attractive since the electrolyte redox system could then be

varied over a wider range to improve conversion efficiencies and perhaps obtain more desirable reaction products (e.g., fuels).

The program emphasis is on developing new electrolyte redox systems and electrode surface modifications which will stabilize the II-VI compounds against photodissolution without seriously degrading the long-term solar response. A cooperative effort involving electrochemistry, synthetic chemistry, and materials characterization provides the mutual feedback necessary to evolve a practical compromise between the interfacial chemistry and the device characteristics. Work is concentrated on the polycrystalline thin films needed for large area, economical solar cells, although single crystal electrodes are used to elucidate some of the surface chemistry. Obviously, much of the chemical knowledge required for redox system design and electrode surface modification is similar, so that considerable synergy exists between these two parallel approaches.

A critical facet of this program involves the development and application of electrochemical photocapacitance spectroscopy (EPS) for in situ characterization of trap levels at semiconductor electrodes. Results obtained to date with this technique are extremely promising.

This broad interdisciplinary approach permits full advantage to be taken of the synergy which exists between the various facets of the program and of the understanding and insight provided by thorough materials characterization. Actual electrochemical solar cells are also built to test concepts and provide additional feedback for further materials development, as well as a better basis for comparing the emerging electrochemical and solid state solar cell technologies.

3.0 TECHNICAL PROGRESS DESCRIPTION

3.1 Development of New Electrolyte Redox Couples

3.1.1 Nonaqueous Redox Couples

To further assess the performance of nonaqueous electrolytes in photoelectrochemical cells, a large number of organic-soluble redox couples were evaluated with CdS, CdSe, and GaAs photoanodes. The redox couples were chosen based on the ready availability of both couple members. Couples with intense colors, such as the vast majority of organic radical species, were not considered. Both one- and two-electron systems were examined. Only two organic solvents appeared to be suitable for PEC use by virtue of their abilities to support the current densities required, i.e., methanol and acetonitrile. Our previous work and that of others in the SERI program support this contention that only these polar, non-viscous solvents show any tangible promise of success in PEC devices.

The one-electron redox couples evaluated were the $Fe^{3+/2+}$ and the $Cu^{2+/1+}$ couples (as the perchlorate and tetrafluoroborate salts, respectively). The two-electron systems included several halide and psuedohalide couples, i.e., I^-/I_3^-, $CN^-/(CN)_2$, $CN^-/Fe(CN)_6^{3-}$, $SCN^-/(SCN)_2$, SCN^-/I_2, and Br^-/I_2, and several sulfur-based systems, i.e., $Et_2NCS_2^-/(Et_2NCS_2)_2$ (the diethyldithiocarbamate, DTC, couple), $\underline{o}\text{-}C_6H_4(SH)(CO_2^-)/[\underline{o}\text{-}C_6H_4(CO_2^-)S]_2$ (the thiosalicylate couple), and S^{2-}/S_n^{2-}. Sodium or tetraethylammonium salts of the anions were typically employed; $(CN)_2$ and $(Et_2NCS_2)_2$ were generated by I_2 oxidation of cyanide and DTC ions, respectively, and $(SCN)_2$ by Br_2 oxidation of thiocyanate ion.

Redox couple concentrations were typically ~ 0.2-0.5 M in reducing agent and ~ 0.05 M in oxidizing agent, and sodium or tetraethylammonium perchlorates were employed as supporting electrolytes (~ 0.1 M). Cells were operated in the two-electrode mode (Pt counter electrode) under tungsten-halogen illumination at ~ 83 mW/cm^2, and the electrolytes were stirred. Observed values of V_{oc} and the fill factor were used as preliminary performance criteria.

By and large, the overall performance of most of these redox couples in acetonitrile or methanol electrolytes was mediocre with respect to PEC use with CdX and GaAs photoanodes. Only those systems which exhibited better-than-average behavior are discussed below.

I^-/I_3^- Couple in Methanol. While corrosive to n-CdSe and dark in color, this redox couple nonetheless afforded reasonable output parameters (comparable to those of the aqueous system), i.e., V_{oc} = 600 mV with a 60-70% fill factor. Sodium counterions seemed to provide better fill factors than the large tetraethylammonium ions; likewise, lower fill factors were observed in acetonitrile (and dimethylformamide). The effect of added charge transfer mediators, e.g., CN^-, Fe^{2+}, 4,4'-bipyridyl, pyridine, ferrocene, and triphenylphosphine, had either adverse or no effect on cell performance.

$SCN^-/(SCN)_2$ Couple in Acetonitrile. Thiocyanogen, $(SCN)_2$, is intermediate in oxidizing ability between I_2 and Br_2, and its solutions are very corrosive to semiconductors. While impractical due to the propensity of $(SCN)_2$ to polymerize on the vessel walls to yellow $(SCN)_x$, V_{oc} values of 700 mV with 70% fill factors were observed with n-CdSe.

$Cu^{2+/1+}$ Couple in Acetonitrile. The copper salts incorporated in the acetonitrile electrolyte were $Cu(ACN)_4BF_4$ and $Cu(BF_4)_2 \cdot xH_2O$. With n-CdSe, V_{oc} values of 800 mV with 75% fill factors were observed, however the photocurrent decayed rapidly, apparently because of formation of a dark layer of Cu_2Se on the electrode surface (no red Se° layer was seen). Consequently, this couple was not considered further, though its use in conjunction with a protective film on the photoanode remains a possibility. The addition of small amounts of Cl^- ion to the electrolyte reduced the V_{oc}.

$Fe^{3+/2+}$ Couple in Acetonitrile. The hydrated perchlorate salts of iron(II) and -(III) were used in acetonitrile, affording red solutions which were apparently light stable. Small amounts of chloride ion, added as tetraethylammonium chloride (TEACl), improved the fill factors somewhat with n-CdS and n-CdSe (with 0.1 M $LiClO_4$ as supporting electrolyte). Figure 1 shows the electrochemical behavior of this couple on Pt and on illuminated n-CdS. With

CdSe photoanodes, the observed V_{OC} was 950 mV with a 75% fill factor, as shown by the power curve in Fig. 2. At a photocurrent density of 10 mA/cm^2, the non-optimized efficiency for this system was 8.5% with 83 mW/cm^2 tungsten-halogen illumination. Power curves for GaAs and CdS photoanodes with the $Fe^{3+/2+}$-ACN electrolyte are given in Figs. 3 and 4. Output parameters for this couple were significantly lower in methanol, dimethylformamide, and DMSO.

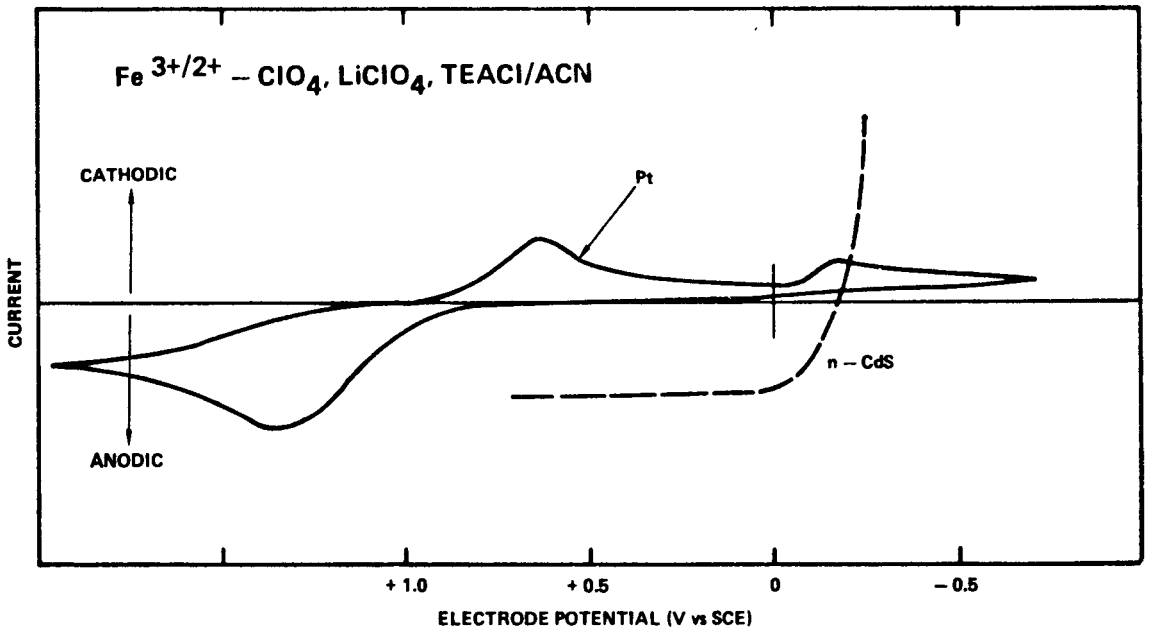

Fig. 1 Voltammetric characteristics of the hydrated $Fe^{3+/2+}$ perchlorate couple on Pt and illuminated CdS in acetonitrile containing 0.1 M $LiClO_4$ and ~ 1 mM Et_4NCl (as a charge transfer mediator).

Although the performance characteristics are impressive, CdX photoanodes corrode in this electrolyte, even at open circuit, presumably because of the oxidizing power of the Fe^{3+} species. The corrosion is not effectively suppressed by use of polypyrrole films. Although the redox reaction is

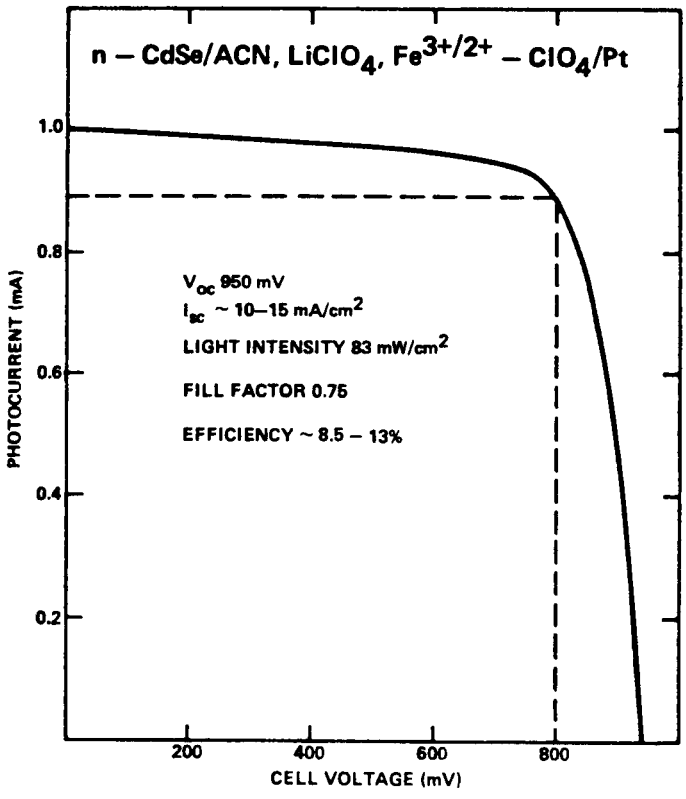

Fig. 2

Power curve for the unoptimized n-CdSe/0.2 M $Fe(ClO_4)_2 \cdot 6H_2O$, 0.05 M $Fe(ClO_4)_3 \cdot 6H_2O$, 0.1 M $LiClO_4$, 1 mM Et_4NCl in acetonitrile/Pt system.

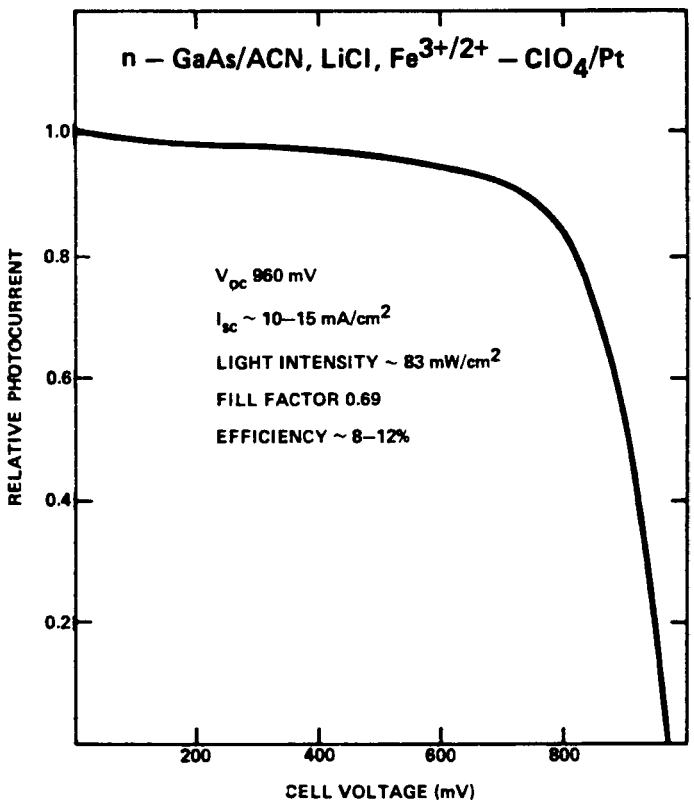

Fig. 3

Power curve for n-GaAs in the same system as for Fig. 2 except 0.05 M Et_4NCl.

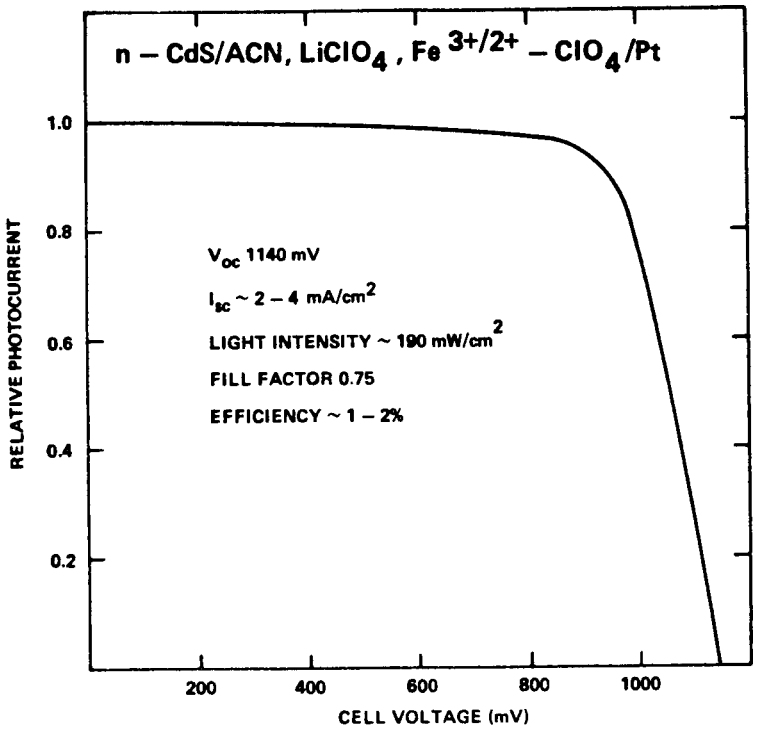

Fig. 4 Power curve for n-CdS in the same system as for Fig. 2.

somewhat irreversible, the net solution composition appears to remain unchanged under PEC operation. Efforts to remove water from these solutions with 3Å molecular sieves were successful to a degree, and resulted in an anodic shift of all the redox waves. Subsequently, V_{OC} values were larger, up to 1150 mV with n-CdSe, but fill factors were poorer, possibly because of very rapid photoanode corrosion.

3.1.2 Comparison with Aqueous Redox Couples

Based on our experience and the available literature data, we feel that organic solvents offer no clear-cut advantage compared to water for PEC use. Of the common nonaqueous solvents, only acetonitrile and methanol appear to provide the solubility for ionic species and low viscosity required for good electrolyte conductivity and adequate mass transport. In at least one

system, i.e., n-CdSe in methanol/$Fe(CN)_6^{3-/4-}$, photodecomposition is almost completely suppressed [22], but the photocurrent is limited by specific adsorption of redox species and, to a lesser extent, increased electrolyte viscosity associated with ion pairing [23]. In some systems, the organic solvent can produce a large shift in the E° value of the couple, as is the case for $Fe^{3+/2+}$ and Cu^{2+}/Cu^{1+} in acetonitrile, so that corrosion of the photoanode is actually enhanced.

It now appears that improvement in PEC performance, compared to that obtained with the aqueous polysulfide system, will require the use of protective films. In this case, the performance characteristics attainable with a particular redox system are more important than the photoanode stabilization provided. Based on this criterion, the following promising redox systems, whose components are readily available, very soluble, and not highly colored, can be identified:

(1) $Fe^{3+/2+}$ perchlorates in acetonitrile with a lithium perchlorate supporting electrolyte and tetraethylammoniuum chloride as a charge transfer mediator;

(2) $Fe^{3+/2+}$ perchlorates in aqueous perchloric acid solution containing lithium chloride as a charge transfer mediator; and

(3) $Fe(CN)_6^{3-/4-}$ in aqueous basic solution.

Performance parameters (open circuit voltages and fill factors) observed with these systems with various single crystal photoanodes are given in Table I. In all cases, attainable conversion efficiencies are in the 10% range. From a performance standpoint, the best system appears to be aqueous $Fe(CN)_6^{3-/4-}$, but the redox couple itself is photolytically unstable so that backside illumination would be required. The $Fe^{3+/2+}$ couple appears to be stable under illumination in both aqueous and acetonitrile solutions.

Table I

Open Circuit Voltages and Fill Factors Attained with Various Photoanodes In Different Redox Electrolytes

Redox System	n-CdS	n-CdSe	n-GaAs
$Fe^{3+/2+}$ - ClO_4	V_{oc} = 1.1 - 1.3 V	0.95 - 1.15	1.0
Acetonitrile	FF = 0.75	0.75	0.7
Aqueous $Fe^{3+/2+}$	V_{oc} = 0.95 V	0.7	0.9
Perchloric Acid	FF = 0.6 - 0.7	0.6 - 0.7	0.7
Aqueous $Fe(CN)_6^{3-/4-}$	V_{oc} = 1.15 V	1.0	1.35
Basic Solutions	FF = 0.8	0.8	0.8

Other redox couples that would be expected to provide high conversion efficiencies include $Cu^{2+/1+}$ fluoroborate in acetonitrile and perhaps the somewhat less efficient I^-/I_3^- couple in water or methanol. Since systems requiring the use of protective films are under discussion, two other strongly oxidizing couples, i.e., aqueous $Ce^{4+/3+}$-ClO_4 (E° = +1.22 V vs SCE) and $Mo(CN)_8^{3-/4-}$ (E° = +0.57 V), should be mentioned. These redox systems, which cover a range of pH values as well as non-aqueous solvents, provide a high degree of flexibility with respect to protective film development.

3.1.3 Stability of the Aqueous $Fe(CN)_6^{3-/4-}$ Couple

Although the aqueous ferro-ferricyanide system has been found to be unstable in sunlight, the possibility has remained that this couple might be used in PEC's employing backside illumination or appropriate filtering to shield the solution from higher energy light. Recently, there has been considerable interest in utilizing the aqueous ferro-ferricyanide couple with polycrystalline n-CdSe photoanodes prepared by various methods, e.g., spray pyrolysis (Chronar), electrodeposition (EIC and Brooklyn College), and evaporation (Grumman); efficiencies up to 10%, which compares favorably with single crystal values (13%), have been obtained.

In the present work, the stability of the aqueous ferro-ferricyanide system under illumination with appropriately-filtered light was evaluated qualitatively. A basic solution (pH 13.2) containing 0.1 M NaOH and 0.25 M each of $Fe(CN_6^{3-/4-}$ was sealed in glass under an argon atmosphere and exposed to 3-1/2 weeks of Southern California sunlight through a 700 nm long-pass filter; other areas of the container were masked with black tape. Although the rate at which the ferro-ferricyanide species decomposed was much slower with the filtered light, fine particles of iron oxide were evident in the solution after the test. This study indicates that the redox couple in aqueous ferro-ferricyanide/n-CdSe systems is decomposed by sub-bandgap light, either directly or as a result of solution heating. Although this result is not encouraging, further studies with somewhat less energetic light are warranted.

3.2 Modification of the Electrode Surface

3.2.1 Electrochemically Generated Organic Polymer Films

The ability of electrochemically-generated conducting polymer films to suppress, at least partially, semiconductor photodegradation is now well-established for polypyrrole [24-28] and for polyaniline [29]. In general, however, long-term stability of such film-coated photoanodes has not been realized for a number of possible reasons, e.g., lack of adherence, permeability to solvent/solute species, and/or gradual loss of conductivity. The causes of these problems and possible solutions have been investigated and are discussed here for polypyrrole, polyaniline, and some new conducting film materials.

Polypyrrole

A summary of our earlier work with polypyrrole has recently been published and a paper is given in Appendix I to provide background information for the present discussion. The apparent permeability of this material to solvent/solute species poses a serious question regarding the long-term stability of electrochemical solar conversion devices employing such films. It was felt that the proper selection of anion associated with the polymer might provide

denser, less permeable films. For this reason, we examined polypyrrole films incorporating a variety of anions, other than the conventional BF_4^-, ClO_4^-, or PF_6^- counterions [30]. This study was facilitated by the discovery that polypyrrole could be potentiostatically deposited from aqueous electrolytes adjusted to pH 1.5-1.9 with strong acids. Deposition on Pt occurs at +0.6 V (vs SCE) for these electrolytes. Conducting films were prepared with chloride, trifluoromethanesulfonate, p-toluenesulfonate, sulfate, and polystyrenesulfonate (PSS) counterions. All such films exhibited the same conducting behavior displayed by the conventional BF_4^- or ClO_4^- films deposited from acetonitrile solution at +0.9 V. The chloride-containing polymer appeared to form the densest and most adherent film on Pt. (The film densities could be compared based on the colors of the films formed from a given amount of charge; the Cl^- films were the darkest). PSS films are apparently different from the others in that the polymeric anion presumably cannot migrate in and out of the film during oxidation/reduction.

In a number of cases, it was observed that the polypyrrole films on Pt, regardless of the counterion, would slowly deactivate (become insulating) when potential cycled in deoxgenated aqueous redox electrolytes over a narrrow range encompassing the redox potential of the couple, e.g., between 0.0 and +0.4 V with pH 7 $Fe(CN)_6^{3-/4-}$ or between +0.2 and +0.7 V with pH 1 $Fe^{3+/2+}$ sulfate. This gradual <u>irreversible</u> decay in the film conductivity was more rapid at neutral and basic pH than in acidic solutions, and was dependent upon the potential limit of the anodic sweep. At specific anodic potentials, the films abruptly became insulating, even in nonaqueous electrolytes; these data are summarized in Table II. In certain instances, however, such as with $Fe^{3+/2+}$ in 11 <u>M</u> LiCl and 1 <u>M</u> HCl, repeated cycling of a polypyrrole/Pt electrode over the redox couple potential regime gave no indication of film passivation, suggesting that the inherent tendency of polypyrrole towards irreversible oxidation may be supressed in some electrolytes.

Table II

Decomposition Potential For Conducting Polymer Films in Various Media

Film	Solvent/Supporting Electrolyte	Decomposition Potential (V vs SCE)
Polypyrrole	Acetonitrile/TEAP or $TEABF_4$	1.65 to 1.75
	Water/0.2 M H_2SO_4	1.1
	Methanol/$LiClO_4$	1.4
Polyaniline	Water/0.2 M H_2SO_4	>1.6
	Acetonitrile/$LiClO_4$	>1.3
Polythiophene	Acetonitrile/$LiClO_4$	1.8
	Water/0.2 M H_2SO_4	1.3

Polyaniline

Polyaniline conducting films were first described by Diaz and Logan [31]. Application to semiconductors was initiated at Rockwell and then investigated further at SERI. A preprint of this work is given in Appendix II. The films are deposited potentiostatically at +0.8 to +1.0 V (vs SCE) from quiescent acidic (pH 0.5-1.5) aqueous solutions containing aniline. Oxidation and reduction of the films are associated with proton elimination and addition and take place reversibly only in acidic aqueous electrolytes of pH < 2. This restricts the redox couples useable with these films to those stable in acidic media, e.g., $Fe^{3+/2+}$. Film electroactivity has also been observed in acetonitrile electrolytes, but is lost in other organic solvents, e.g. methanol. The films dissolve in DMSO and DMF. Polyaniline appears to be more stable than polypyrrole since the conductivity of polyaniline films is retained at potentials positive of the oxygen evolution potential (see Table II).

Polyaniline films have been photoelectrochemically deposited onto illuminated CdSe and Si photoanodes (as well as p-type semiconductors in the dark), but not onto n-GaAs, and, like polypyrrole, enhance the semiconductor stabililty without significantly interferring with charge transfer. In opera-

tion, however, the photocurrent for film-coated electrodes gradually decays, more rapidly in the case of n-CdSe compared to n-Si. The photocurrent decay presumably results from porosity, pinholes, or imperfect adhesion and subsequent semiconductor photodecomposition. A possible source of this problem may be simultaneous photodecomposition of the illuminated photoanodes during the polyaniline deposition process, resulting in decomposition products forming at the semiconductor/polymer interface or within the polymer itself. More recently, superior film deposition was found to take place on these semiconductor photoanodes at very low current densities (low illumination) of about 50 $\mu A/cm^2$. Under these conditions, noteably less photodecomposition of the semiconductor took place and more uniform polymer films were laid down relative to those deposited under the "standard" 80-100 mW/cm^2 illumination. In any case, polyaniline appears to be unsuitable for long-term PEC use, at least with n-CdSe and aqueous electrolytes.

Polythiophene

The sulfur analogue of pyrrole, thiophene, $\overline{CH(CH)_3S}$, can be made to polymerize under certain conditions to form a partially conducting polymer film, polythiophene. On Pt in acetonitrile containing 0.2 M trifluoromethanesulfonic (triflic) acid, thiophene oxidatively polymerizes at ~ +1.5 V to form a brown film. The resulting polythiophene-triflate polymer displays a broad featureless redox wave beginning at ~ +0.1 V in aqueous and acetonitrile electrolytes.

Polythiophene is much less stable than polypyrrole and becomes insulating more rapidly under the same conditions. In addition, it appears to be less conducting, particularly with respect to reducing cationic species in solution. For example, with aqueous $Fe^{3+/2+}$, an oxidation wave for $Fe^{2+} \rightarrow Fe^{3+}$ was observed on polythiopene/Pt, but no cathodic current was seen on reverse potential scan. With ferrocene in acetonitrile, only a modest reduction current was observed with this electrode, correspondingly to $Cp_2Fe^+ \rightarrow Cp_2Fe^\circ$. Only with aqueous $Fe(CN)_6^{3-/4-}$ anions, which presumably become incorporated in the film, was a normal voltammetric wave observed. Like polypyrrole, polythiophene irreversibly oxidizes to an insulator (Table II).

All attempts to photoelectrochemically deposit polythiophene onto n-CdS and n-CdSe from the acetonitrile/thiophene/triflic acid electrolyte were unsuccessful. Apparently, the deposition potential of +1.5 V is too positive for these photoanodes so that photodegradation predominates. Nonetheless, some properties of this material, particularly the diode behavior alluded to above, and its purportedly more facile electrodeposition from 2,2'-dithienyl [32], possibly warrant further investigation.

3.2.2 Transition Metal Oxide Films

Since many transition metal oxides are extremely stable electrochemically, i.e., form passive films, and can be made highly conducting by appropriate doping, they are prime candidate materials for photoanode protective films. Oxide structures are also relatively dense compared to most organic polymers and represent a closer lattice match to semiconductor substrates. In addition, the valence bands of some transition metal oxide semiconductors favorably overlap those of narrow-band-gap materials, which should facilitate transport of photogenerated holes to electrolyte species. The major objection to the use of oxide films has been the difficulty associated with applying them to suitable substrates.

Recently, a new electrochemical method for preparing a number of conducting transition metal oxide/hydroxide films was developed in our laboratory. In this method, the potential of the substrate electrode was cycled/controlled in a buffered solution containing metal ions of the oxide to be deposited. Preprints describing this method and the properties of the resulting films are given in Appendices III and IV. For the ruthenium oxide, a novel organometallic precursor was employed which cleanly decomposed electrochemically.

The metal oxide films prepared by the electrochemical method are conducting to varying degrees in aqueous and nonaqueous solutions. While the electrodeposited copper oxide is semiconducting (p-type), the nickel, cobalt, iron, manganese, and ruthenium oxides behave more or less like the organic conductors polypyrrole and polyaniline. For example, the cobalt, manganese,

and ruthenium oxides can be grown to thicknesses in the 1 μm range with no decay in the deposition current; on the other hand, the iron oxide rapidly becomes insulating at thicknesses > ~ 300Å.

Our initial attempts to electrochemically deposit the anodic metal oxides onto illuminated n-type semiconductors met with only partical success, apparently because of simultaneous photodecomposition of the substrate materials in the aqueous solutions. Recently, much better films have been obtained by utilizing lower illumination intensities and optimizing the metal ion concentrations in the deposition solutions - higher concentrations (~ 0.2 - 0.25 M) than those given in Table 1 of Appendix III were found to be advantageous. Deposition is sluggish in more concentrated solutions, possibly because of greater M^{2+} complex formation.

Typically, deposition onto n-CdS or n-CdSe was performed by biasing the electrode at constant potential (+0.4 V vs SCE) in the appropriate solution and adjusting the light intensity to produce current densities of 50 μA/cm^2. Film thicknesses in most cases were nominally ~ 2000-4000Å corresponding to the passage of about 50-100 mC/cm^2 of charge. Attainable thickness for the iron oxide films is much smaller because of the insulating nature of this material. Although the potential scanning technique used for the nickel oxide deposition on Pt (Appendix III) is not convenient for deposition on photoanodes, a cathodic deposition procedure (from nickel nitrate solution) was found to work well. Because of the instability of electrodeposited copper oxide in aqueous electrolytes, deposition on this material on semiconductors has not been investigated.

Most of the oxide films can be deposited onto n-CdS and n-CdSe. For n-GaAs, anodic oxide deposition was not observed, apparently because of substrate photodecomposition. The colors of the films are much less intense than those of polypyrrole or polyaniline so that thicker oxide films can be used. Adherence of the oxides on CdS and CdSe is excellent -- far superior to that of polypyrrole.

Thus far, the behavior of n-CdSe coated with metal oxide films has been investigated only in the aqueous $Fe(CN)_6^{3-/4-}$ (pH 13) electrolyte. With rela-

tively thin iron, cobalt, and manganese oxide films, the initial overall performance of the photoanodes approaches that of the naked semiconductors. With very thick films, photovoltages and photocurrents decrease accordingly, as is the case with polypyrrole. The initial photoanode stability is dramatically enhanced relative to that of the bare electrode, although after an hour or two the photocurrent begins to decay slowly, indicating film failure. Failure may be due to chemical reaction of the film with the ferrocyanide species (and/or possibly free cyanide) in the electrolyte. Photoanodes with cathodically generated nickel hydroxide films exhibited very poor photoresponse, probably because of adverse surface modifications (surface state formation) effected by the cathodic bias.

Future studies with conducting metal oxide films will involve redox electrolytes for which film stability is expected to be better than for the aqueous $Fe(CN)_6^{3-/4-}$ (pH 13) solution. Nonaqueous solvent systems are particularly attractive since the films appear to be less reactive in such systems. Heat treatment of the deposited oxide films prior to incorporation in PEC's, catalytic effects of the films with regards to oxygen or halogen evolution, and behavior of oxide films on other semiconductor substrates, (e.g., n-Si and p-type materials) will also be examined.

3.2.3 Evaporated Conducting Films - Lutetium Diphthalocyanine

Another approach to obtaining protective conducting films on narrow-band-gap semiconductors involves vapor deposition of suitable film materials. With this technique, problems associated with degradation and contamination of the interface during deposition should be minimal. We have initiated studies with the multicolor electrochromic material lutetium diphthalocyanine [33], $LuPc_2$, as the conducting film; its structure is shown in Fig. 5. While the partial stabilizing ability of "conventional" planar phthalocyanine films, e.g., of CuPc and H_2Pc, on n-Si in PECs has been demonstrated [34,35], the intense colors and low conductivities of these films restrict the attainable photocurrents to rather low values. The pale green $LuPc_2$, on the other hand, is a fast electrochromic and, like most phthalocyanines, exhibits remarkable chemical stability. $LuPc_2$ can be doped oxidatively or reductively.

STRUCTURE OF RARE EARTH DIPHTHALOCYANINES, $LnPc_2$

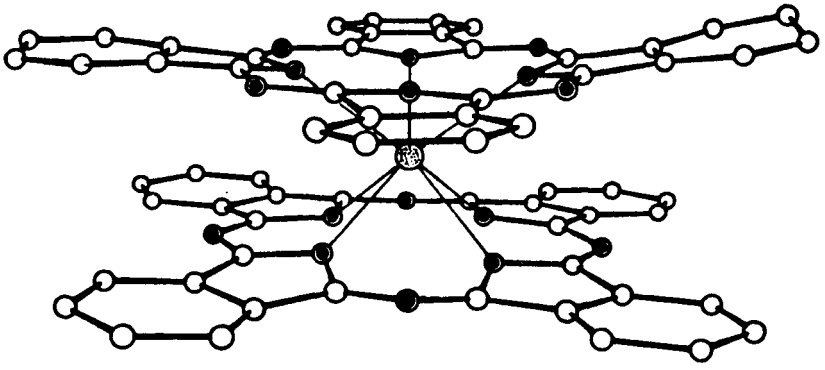

Ln (III)
C
N

M. Tsutsui, et al., J. Am. Chem. Soc., 1980, 102, 4835.

Fig. 5 Structure of the rare earth diphthalocyanines.

Lutetium diphthalocyanine was prepared using a modification of the published procedures [33,36,37]. Lutetium acetate (2.0 g) and phthalonitrile (7.0 g) were placed in a 50 ml round-bottom flask which was fitted with a reducing adaptor through which a loosely-fitting thermometer was inserted so as to nearly touch the bottom of the flask. The flask was maintained (with a heating mantle) at the boiling point of the phthalonitrile (~ 290°) for 3 h. The resulting dark solid was treated in a Soxhlet apparatus with methanol and acetone (extracts discarded) and then extracted with chloroform (~ 4 days). The green chloroform extract was evaporated to dryness, and the solid stirred with warm (60°) acetic anhydride, followed by Soxhlet treatment with methanol and acetone. The yield of crude dark green $LuPc_2$ was 1.60 g. This material was further purified by dissolving in 300 ml of boiling chloroform, filtering, adding 300 ml of

toluene to the filtrate, and boiling again. The hot mixture was filtered and the filtrate rapidly passed through a 10-12 cm column of silica gel. The resulting solution was reduced in volume with a rotary evaporator at room temperature to afford, after filtration, black, highly crystalline $LuPc_2$.

The purified $LuPc_2$ was evaporated onto conducting and semiconducting substrates in a Veeco V-300 evaporator. The apparatus was evacuated to $\sim 10^{-6}$ Torr and the alumina crucible containing the $LuPc_2$ ($\sim$ 10 mg) was heated indirectly to $\sim$ 450°. Sublimation of the compound yielded uniform pale green films on the substrate electrodes atop a glass chimney 15 cm above the crucible. Typical thicknesses were in the 1500-2000Å region and were monitored with a standard crystal control device.

$LuPc_2$ films deposited onto conducting SnO_2 glass display their characteristic electrochromic properties in aqueous Na_2SO_4 solution, changing from green to red at $\sim$ +0.6 V (vs SCE) and from green to blue at $\sim$ -0.3 V. In 0.1 M NaOH containing 0.01 M $Fe(CN)_6^{4-}$ a reversible ferri-ferrocyanide redox wave is observed with the film coated SnO_2.

$LuPc_2$ films were also deposited onto CdSe and GaAs photoanodes and examined in PECs at AM1 light intensities. With GaAs substrates, the films rapidly peeled from the semiconductor surfaces within minutes of operation in aqueous redox electrolytes. With n-CdSe, on the other hand, film adherence was very good, and the coated electrodes were noteably more stable than bare photoanodes. Very slow decay in the photocurrents was observed with the n-CdSe/$LuPc_2$ sysems, however, in aqueous $Fe^{3+/2+}$ (pH 1) and $Fe(CN)_6^{3-/4-}$ (pH 13) solutions. The nearly equivalent decay rates observed seemed to be independent of the electrolyte composition, suggesting either passivation of the organic film and/or semiconductor photodecomposition. With respect to the latter, the films could be removed with chloroform and a cotton swab, and upon further PEC operation the electrodes showed no visual buildup of the normal photodecomposition products (Se°, $Cd_2Fe(CN)_6$, etc.) even after prolonged use, although the photocurrent did continue its slow decline. This indicates that some chemical reaction of the $LuPc_2$ and the CdSe surface does occur, yielding a rather impervious layer (reddish under reflected light) which suppresses the normal photodecomposition.

Low photocurrents associated with the "conventional" phthalocyanine-coated semiconductors [35] have been attributed to the high resistance of these materials, which are typically in the range 10^{-9} to 10^{-11} ohm^{-1} cm^{-1} [38]. Although the resistivity of $LuPc_2$ is much less, on the order of 10^{-4} ohm^{-1} cm^{-1} [39], photocurrent reduction, although not as severe, is also observed in this case. Recently, Bard, et. al. have shown that iodine doping of the "conventional" phthalocyanine films enhances their conductivity markedly, resulting in much larger currents [35]. Additional improvements in stability were observed by these workers for concentrated electrolytes, e.g., 11 M LiCl, for which the water activity is decreased. We plan to investigate the implications of these findings for $LuPc_2$ films, and to evaluate the use of nonaqueous redox systems. The pale color, higher conductivity, and unique interaction with n-CdSe surfaces make $LuPc_2$ a significantly better choice than the "conventional" phthalocyanines for semiconductor stabilization.

3.3 Electrochemical Photocapacitance Spectroscopy

Electrochemical photocapacitance spectroscopy (EPS) is a new characterization method (being developed under this program) which has several inherent advantages and the potential, recently demonstrated [40,41], of filling a long-standing need in the field of semiconductor electrochemistry for an *in situ* method of quantitatively detecting and characterizing surface states and bulk levels at the semiconductor-electrolyte interface. First of all, charged or discharged states produced by phototransitions generally accumulate in the space charge layer or at the interface causing an integral effect on the capacitance so that the sensitivity of EPS is enhanced in comparison to techniques based on simple photocurrent measurements. Compared to the analogous solid-state photocapacitance technique [42-46], EPS is also more sensitive since leakage currents can be considerably reduced in electrochemical systems by adjusting the availability of electronic states in the electrolyte, and the monolayer-sharp junction with transparent electrolytes permits more light to be focused on the area of interest, i.e., the space charge region. In addition, EPS is relatively simple to perform, compared to techniques like deep level transient spectroscopy (DLTS), and with the proper choice of electrolyte is non-destructive. On the

other hand, since EPS is an in situ electrochemical technique, the electrolyte can be chosen to permit characterization of electronic states associated with the semiconductor-electrolyte interface or passive films, e.g., oxides.

The EPS method and some results for n-GaAs are described in a recent publication [41], which is reproduced in Appendix V. In this section, results for n-CdSe, both single crystal and polycrystalline, are presented.

Figure 6 shows an EPS spectrum for a photoetched single crystal of n-CdSe in a basic aqueous electrolyte. Note that this spectrum was recorded in less than 15 min. Electrode potentials reported here are given relative to the flatband potential (U_{fb}). Three capacitance increases/ plateaux, associated with transitions from donor states at 1.04, 1.21 and 1.34 eV to the conduction band, are evident. A capacitance decrease near the bandedge (at 1.60 eV), corresponding to a transition from the valance band to a state ~ 0.15 eV below the conduction bandedge, is also resolved.

The probable origin of these levels can be ascertained by comparison of the EPS results with the vacuum surface photovoltage data for single crystal n-CdSe reported by Brillson [47]. Figure 7 shows an EPS spectrum for chemically-etched single crystal n-CdSe (curve 1), and surface photovoltage spectra for oxygen-adsorbed* (curve 2) and vacuum-cleaved (curve 3) surfaces. Note that the surface photovoltage spectrum for the oxygen-adsorbed surface and the EPS spectrum are very similar, indicating that the same bandgap states are involved. The 1.04 eV transition, and possibly the transition at 1.2 eV (not resolved by the vacuum technique), must involve interface states associated with oxygen adsorption since no change in surface photovoltage was observed for the vacuum-cleaved CdSe (curve 3) in this energy range. The 1.34 eV transition is apparently intrinsic to CdSe since it was detected by Brillson for both vacuum-cleaved and oxygen-adsorbed CdSe crystals. EPS data for n-CdSe single crystals with various surface pretreatments indicate that both the 1.04 and 1.34 eV transitions are associated with surface states. For example, although the same

*Such a surface gave results very similar to those for an etched surface and might be expected to be comparable to that in an aqueous solution.

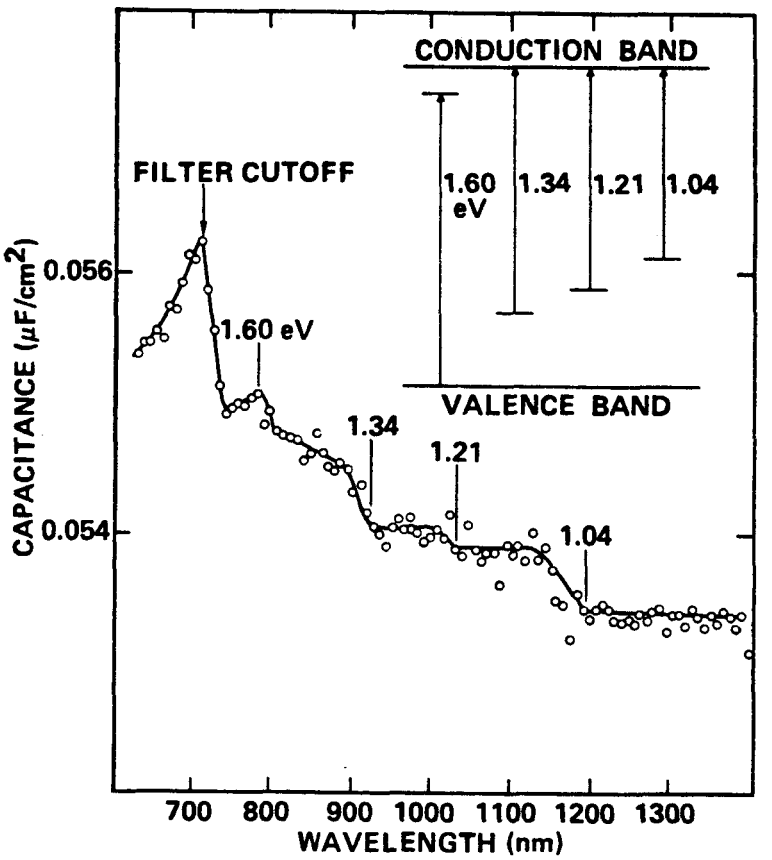

Fig. 6. EPS spectrum (5 kHz) and associated energy levels/phototransitions for a photoetched n-CdSe single crystal (0.9 V vs U_{fb}) in aqueous 0.5 M KOH solution.

transitions are observed for both photoetched (Fig. 6) and chemically-etched surfaces (Fig. 7), the 1.04 and 1.34 eV states are in much higher concentrations (larger capacitance changes) after the latter surface pretreatment.

Although the capacitance decrease occurring just below the bandedge (at ~ 1.6 eV) is not always clearly resolved in EPS spectra because of interference from band tailing, the state responsible (~ 0.2 eV below the conduction band-edge) always seems to be present in CdSe, at least in small concentrations, and is noteworthy. Brillson [47] found that argon-bombardment enhances the corresponding feature in surface photovoltage spectra, indicating that the state involved is associated with a lattice defect. As shown below by EPS, this state

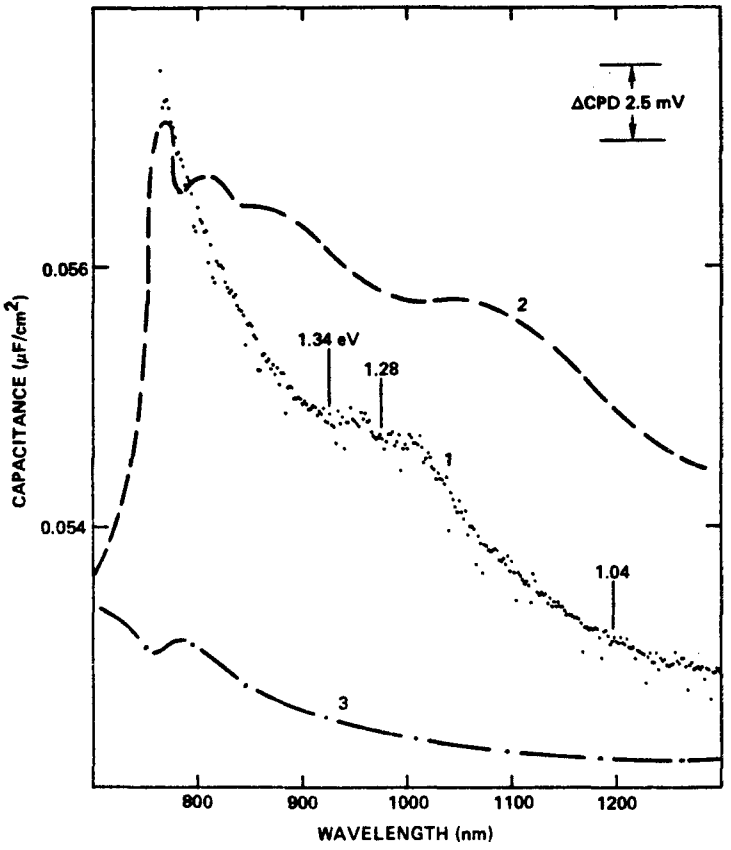

Fig. 7. Surface photovoltage spectra for oxygen-adsorbed (70% coverage) and vacuum-cleaved (LEED-ordered) single crystal n-CdSe (after L. J. Brillson [47]) and an EPS spectrum (5 kHz) for chemically-etched single crystal CdSe in 0.5 M KOH solution.

is a donor-type surface state which is present in large concentrations in polycrystalline material prepared under some conditions.

EPS data for n-CdSe in aqueous solutions also correlates extremely well with other solid-state literature data for oxygen adsorbed surfaces [48-53]. Another example is given in Fig. 8, which shows the EPS spectrum from Fig. 7 on the same graph with photocapacitance data reported by Ture et al. [48] for an aged Au-CdSe Schottky barrier device. Again, the similarities in the two spectra are striking; the same shifts in onset energies for the various transitions is not suprising considering the differences in environment at the

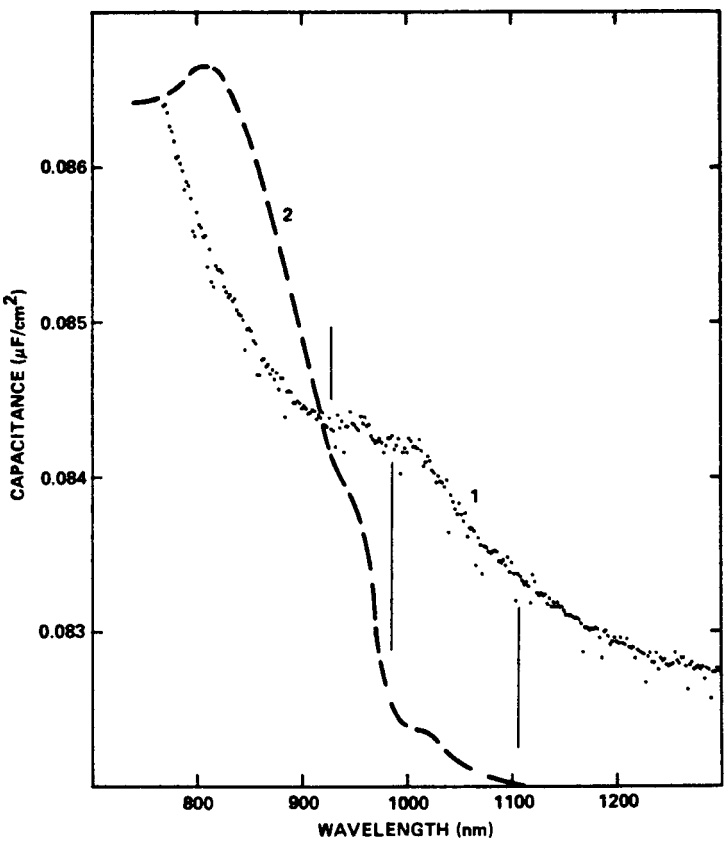

Fig. 8. Comparison of the EPS spectrum from Fig. 7 with a photocapacitance spectrum for an aged Au-CdSe Schottky barrier device (after I. E. Ture, G. J. Russell, and J. Woods, Int. Conf. II-VI Comp. Semicond., BACG, Durham, England, Apr. 21-30, 1982).

two interfaces. It is important to note that these solid-state workers showed that the aging process for their devices involved conversion of the CdSe surface from its normal hexagonal structure to a cubic form, which readily chemisorbs oxygen. It was found that the aging process could be greatly accelerated by polishing the crystal, which produces a cubic surface layer.

Figure 9 shows EPS spectra in 0.5 M KOH for a single crystal n-CdSe after polishing on 1 μm grit without subsequent etching. Although the onset energies are shifted slightly, it is evident that the principal states observed for the etched surfaces (1.04, 1.34 and 1.6 eV) are also present for the polished surfaces, although in larger concentrations. That all of these states

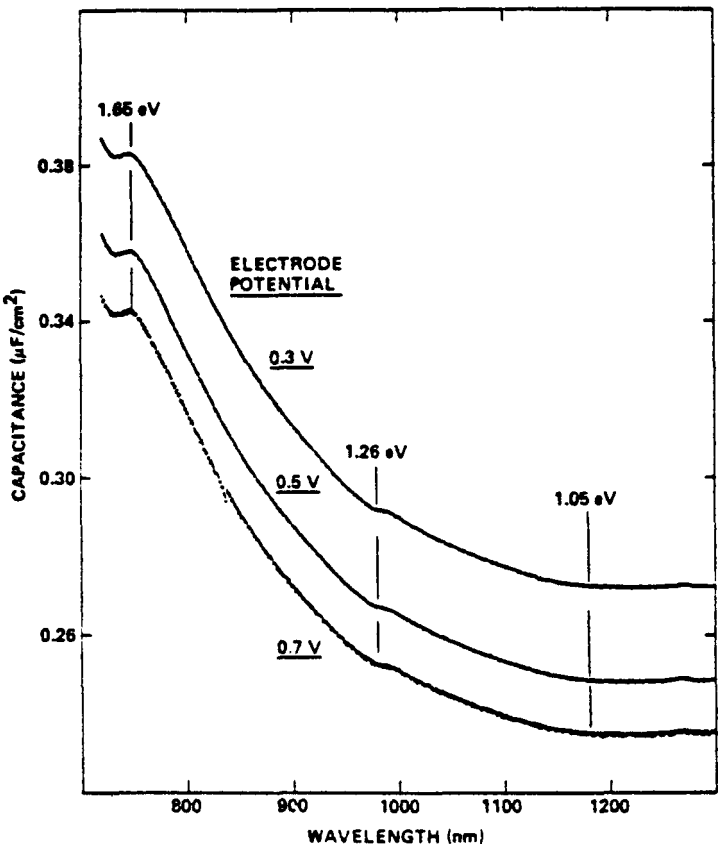

Fig. 9. EPS spectra (5 kHz) for a polished (1 μm) n-CdSe single crystal at various bias voltages in 0.5 M KOH.

reside at the interface is supported by the insensitivity of the corresponding capacitance changes to the electrode potential (Fig. 9).

Figure 10 shows EPS spectra measured in acetonitrile solution for photoetched n-CdSe single crystals from two different batches of material. From spectrum #1 (same material as for studies discussed above), it is evident that the same principal surface states, although shifted to slightly lower energies, are also present in the nonaqueous solvent. This indicates that the CdSe surface structure formed by etching in aqueous solutions, including the chemisorbed oxygen, is reasonably stable in the nonaqueous solvent. For material #2, the 1.40 eV transition is apparently enhanced and a capacitance decrease, corresponding to a transition from the valance band to a bandgap state, is observed

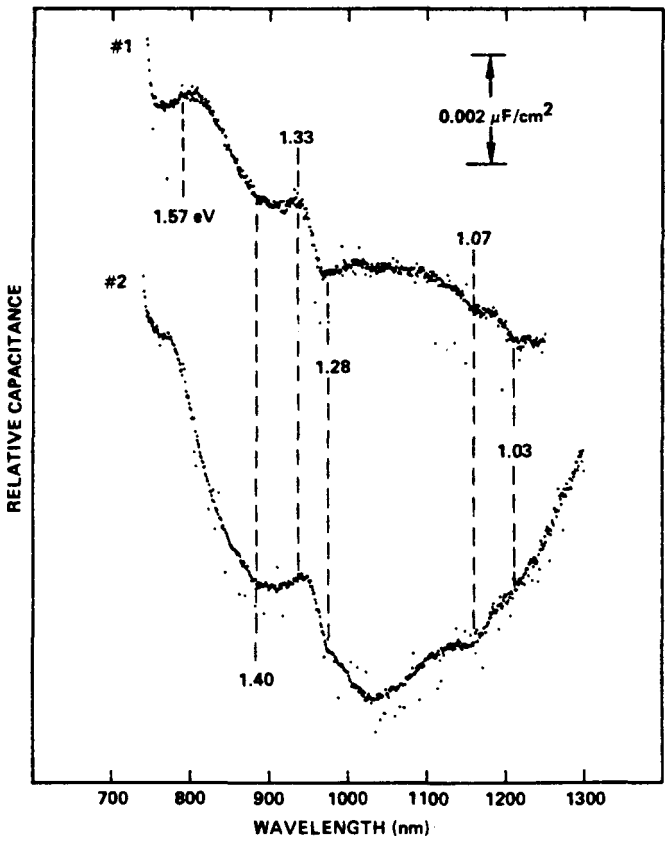

Fig. 10 EPS spectra (7 kHz) in acetonitrile (0.1 M Et_4NClO_4) for photoetched n-CdSe single crystals from two batches of material (1.1 V vs U_{fb}).

at longer wavelengths; the observed "tail" is superimposed on the normal 1.0 eV transition. This long-wavelength tail is also observed for material #2 in aqueous solvents and is apparently associated with excess selenium in the crystal.*

At less positive potentials, significant CdSe surface reactions do occur in acetonitrile solution. This is illustrated in Fig. 11, which

*Photoetching in aqueous sodium sulfate solutions, which is known to produce a selenium layer on CdSe surfaces, greatly enhances the magnitude of the long-wavelength capacitance decrease.

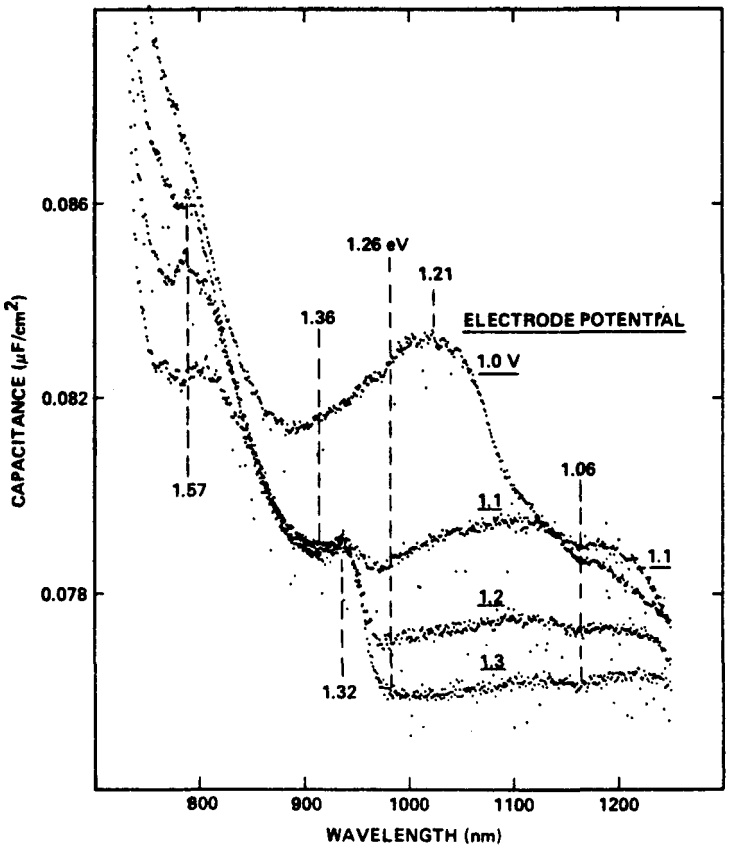

Fig. 11 EPS spectra (7 kHz) in acetonitrile (0.1 M Et_4NClO_4) for a photoetched n-CdSe single crystal as a function of electrode potential.

shows EPS spectra for an n-CdSe single crystal as a function of electrode potential. Normal spectra are observed at more positive potentials. As the electrode potential is decreased, however, the 1.26 eV transition slowly disappears and a capacitance peak appears (1.21 eV). These spectral changes can be explained in terms of the reaction scheme shown in Fig. 12. Apparently, the relatively discrete surface state at ~ 1.2 eV below the conduction bandedge can be electrochemically reduced to form a diffuse surface state species lying at about 0.6 eV. The broad increase in capacitance, whose onset at longer wavelengths is inaccessible, would then correspond to a transition from the state to the conduction band, whereas, the complementary transition would be responsible for the capacitance decrease that results in a peak.

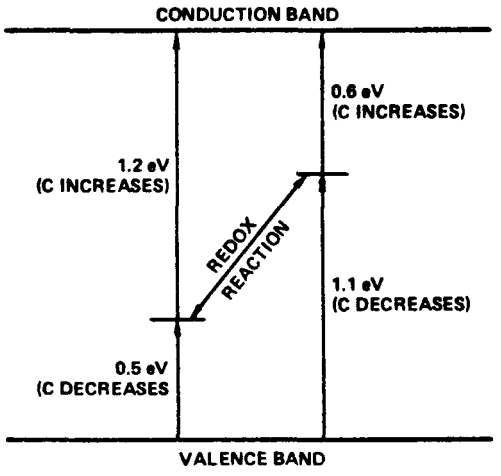

Fig. 12 Energy level diagram illustrating the predominant n-CdSe interface states in acetonitrile solution.

Polycrystalline Materials

The applicability of EPS for characterization of polycrystalline films has also been established. The most significant result is that n-CdSe prepared by co-evaporation of the elements at low substrate temperature [54] contains an appreciable concentration of an electron trap which is found in, at most, small concentrations in single crystals and in film material prepared at a high substrate temperature. This trap apparently lies at ~ 0.2 eV below the conduction band and is detected as a sharp decrease in capacitance at 1.5 eV (Fig. 13), indicating a transition from the valence band to the trap. As the electrode potential is decreased, approaching the flatband potential (U_{fb}), a drastic change in the EPS spectrum occurs. As shown by the spectrum in Fig. 14 (taken at 0.5 V vs U_{fb}), the 1.5 eV transition disappears, apparently because the Fermi level is sufficiently high at this potential to populate the trap so that the transition is no longer possible. In this case, the EPS spectrum is similar to that obtained for single crystal material.

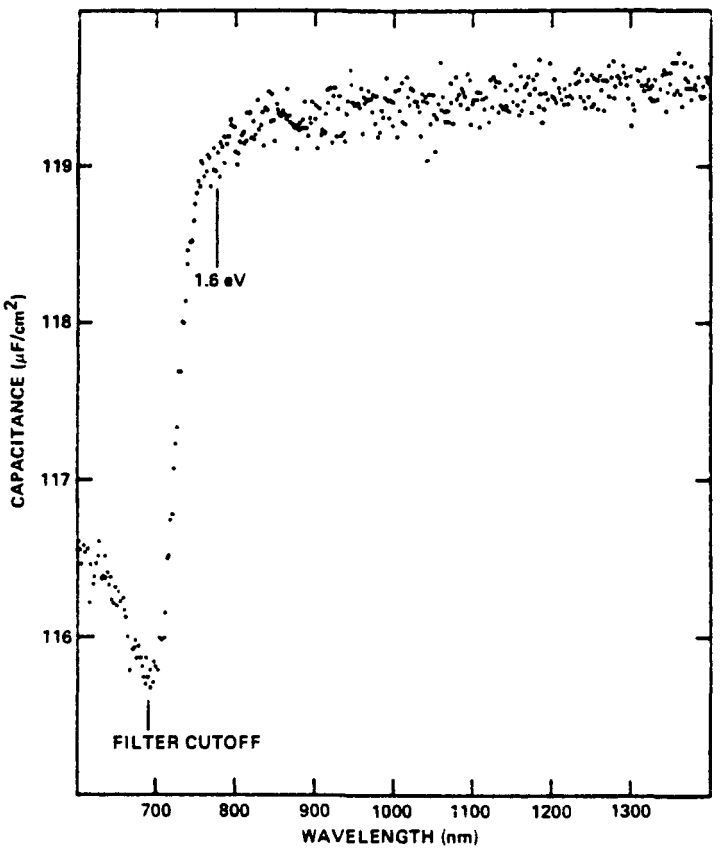

Fig. 13 EPS spectrum for a low-substrate-temperature n-CdSe film electrode at 0.9 V vs U_{fb} in 0.5 M KOH solution.

The implication of these results is that the trap level detected for the low-substrate-temperature material is responsible for the observed limitation of the attainable open circuit voltage [54], and may also limit the photocurrent.

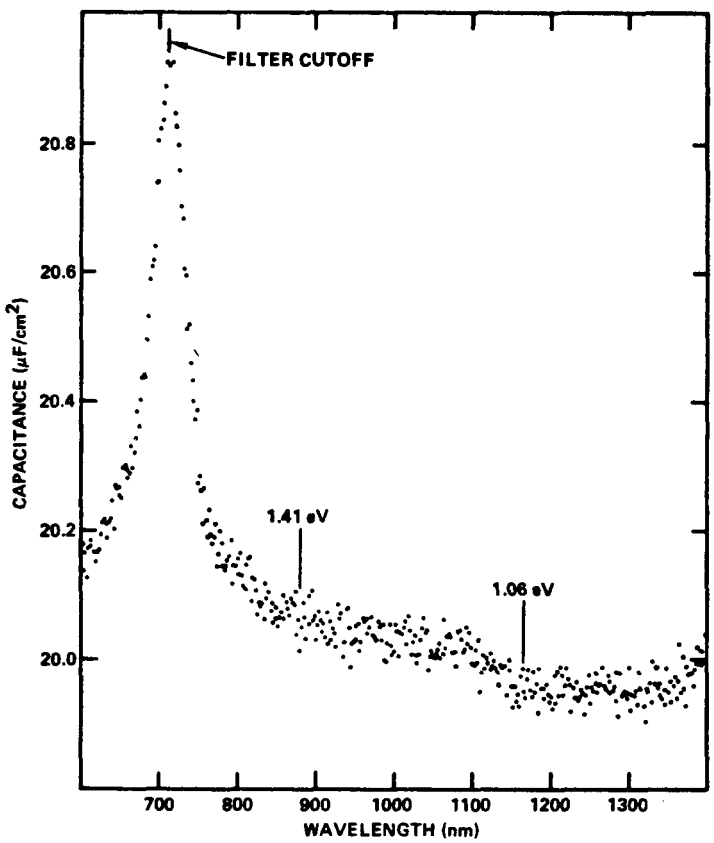

Fig. 14 Same as Fig. 13 except at 0.5 V vs U_{fb}.

4.0 REFERENCES

1. R. Noufi, P. Kohl, and A. J. Bard, J. Electrochem. Soc., 125, 375 (1978).

2. A. B. Ellis, S. W. Kaiser, and M. S. Wrighton, J. Am. Chem. Soc. 98, 1635 (1976).

3. A. B. Ellis, S. W. Kaiser, and M. S. Wrighton, ibid., p. 6418.

4. A. B. Ellis, S. W. Kaiser, and M. S. Wrighton, ibid., p. 6855.

5. A. B. Ellis, S. W. Kaiser, J. M. Botts and M. S. Wrighton, ibid., 99, 2839 (1977).

6. G. Hodes, J. Manassen, and D. Cahen, Nature (London), 261, 403 (1976).

7. G. Hodes, D. Cahen, and J. Manassen, ibid., 260, 312 (1976).

8. J. Manassen, G. Hodes, and D. Cahen, J. Electrochem. Soc, 124, 532 (1977).

9. B. Miller and A. Heller, Nature (London), 262, 680 (1976).

10. A. Heller, K. C. Chang, and B. Miller, J. Electrochem. Soc., 124, 697 (1977).

11. T. Inoue, T. Watanabe, A. Fujishima, K. Honda, and K. Kohayakawa, ibid., 124, 719 (1977).

12. H. Minoura, T. Oki, and M. Tsuiki, Chem. Lett., 1279 (1976).

13. Y. G. Chai and W. W. Anderson, Appl. Phys. Lett, 27, 183 (1975).

14. H. Gerischer, J. Electroanal Chem., 58, 263 (1975).

15. H. Gerischer and J. Gobrecht, Ber. Bunsenges. Physik. Chem., 80, 327 (1976).

16. K. C. Chang, A. Heller, B. Schwartz, S. Menezes, and B. Miller, Science, 196, 1097 (1977).

17. R. Noufi, P. Kohl, J. Rogers, Jr., J. White, and A. J. Bard, J. Electrochem. Soc., 126, 949 (1979).

18. D. Cahen, G. Hodes, and J. Manassen, J. Electrochem. Soc., 125, 1623 (1978).

19. A. Heller, J. P. Schwartz, A. G. Vadinsky, S. Menezes, and B. Miller, J. Electrochem. Soc., 125, 1156 (1978).

20. (a) H. Gerischer and J. Gobrecht, Ber. Bunsenges. Phys. Chem., 82, 520 (1978); (b) H. Gerischer and W. Minalt, Electrochim. Acta., 13, 1239 (1968); (c) H. Gerischer, J. Electroanal. Chem., 82, 133 (1977).

21. B. A. Parkinson, A. Heller, and B. Miller, Appl. Phys. Lett., 33, 521 (1978).

22. R. Noufi, D. Tench and L. F. Warren, J. Electrochem, Soc., 127, 2709 (1980).

23. R. Noufi, D. Tench and L. F. Warren, J. Electrochem. Soc. 128, 2363 (1981).

24. R. Noufi, D. Tench and L. F. Warren, J. Electrochem. Soc., 127, 2310 (1980).

25. R. Noufi, D. Tench and L. F. Warren, J. Electrochem. Soc., 128, 2596 (1981).

26. R. Noufi, A. J. Frank and A. J. Nozik, J. Am. Chem. Soc., 103, 1849 (1981).

27. T. Skotheim, I. Lundstrom and J. Prajza, J. Electrochem. Soc., 128, 1625 (1981).

28. F. - R. F. Fan, B. L. Wheeler, A. J. Bard and R. Noufi, J. Electrochem. Soc., 128, 2042 (1981).

29. R. Noufi, A. J. Nozik, J. White and L. F. Warren, Extended Abst. 561, Electrochem. Soc. Meeting, Denver, CO, Oct. 11-16, 1981.

30. A. F. Diaz, K. K. Kanazawa and G. P. Gardini, J. Chem. Soc. Chem. Commun., 635 (1979).

31. A. F. Diaz and J. A. Logan, J. Electroanal. Chem., 111, 111 (1980).

32. A. F. Diaz, private communcation.

33. B. Walton, B. Ely and G. Elliott, J. Electrochem. Soc., 128, 2479 (1981).

34. Y. Nakato, M. Shioji and H. Tsubomura, J. Phys. Chem., 85, 1670 (1981).

35. P. Leempoel, M. Castro-Acuna, F-R. F. Fan, and A. J. Bard, J. Phys. Chem., 86, 1396 (1982).

36. A. G. MacKay, J. F. Boas, and G. J. Troup, Austr. J. Chem., 27, 955 (1974).

37. A. T. Chang and J-C. Marchon, Inorg. Chim. Acta Lett., 53, L241 (1981).

38. K. Kasuga and M. Tsutsui, Coord. Chem. Rev., 32, 67 (1980).

39. R. Noufi, private communication.

40. R. Haak, C. Ogden and D. Tench, Proc. Electrochem. Soc. Sym. on "Measurement Techniques for Photoelectrochemical Solar Cells/Photoelectrochemical Processes," Denver, CO, Oct. 11-16, 1981.

41. R. Haak, C. Ogden and D. Tench, J. Electrochem. Soc., 129, 891 (1982).

42. A. A. Gutkin, M. B. Kagan, D. N. Nasledov, B. A. Kholev and T. A. Shaposhnikova, Soviet Phys.-Semicond., 5, 1006 (1971).

43. F. D. Hughes, Acta Electonica, 15, 43 (1972).

44. H. Kukimoto, C. H. Henry and F. R. Merritt, Phys. Rev. B, 7, 2486 (1973).

45. K. Sakai and T. Ikoma, Appl. Phys., 5, 165 (1974).

46. D. Bois, J. Physique, 35, C3-241 (1974).

47. L. J. Brillson, Surf. Sci., 69, 62 (1977).

48. J. E. Ture, G. J. Russell and J. Woods, Int. Conf. II-VI Comp. Semicond., BACG, Durham, England, Apr. 21-30, 1982.

49. C. Manfredotti, A. Rizzo, L. Uasanelli, S. Galassini and L. Ruggiero, J. Appl. Phys., 44, 4563 (1973).

50. E. Guesne, C. Sebenne and M. Balkanski, Surf. Sci., 24, 18 (1971).

51. R. L. Consigny and J. R. Madigan, Solid-State Electron., 13, 113 (1970).

52. B. A. Kulp, J. Appl. Phys., 37, 4936 (1966).

53. R. H. Bube and L. A. Barton, J. Chem. Phys., 29, 128 (1958).

54. J. Reichman and M. A. Russak, J. Electrochem. Soc., 128, 2025 (1981).

APPENDIX I

Paper on electrogenerated polypyrrole films published in the Journal of the Electrochemical Society, 128, 2596 (1981).

Protection of Semiconductor Photoanodes with Photoelectrochemically Generated Polypyrrole Films

Rommel Noufi*,[1] Dennis Tench,* and Leslie F. Warren*

Rockwell International, Microelectronics Research and Development Center, Thousand Oaks, California 91360

ABSTRACT

Results are presented which show that photoelectrochemically generated polypyrrole films protect semiconductor photoanodes (*e.g.*, Cd chalcogenides, GaAs, and Si), from degradation while permitting electron exchange between the semiconductor and the electrolyte. The performance characteristics and stability of such film-covered photoelectrodes are discussed.

In an earlier brief communication (1), we described the electrochemical generation of conducting polypyrrole films on n-GaAs and the characteristics of the resulting photoanodes. It was demonstrated that such polymer films inhibit photodegradation of the semiconductor, presumably by impeding ion/solvent transport. Good photoanode performance characteristics, from an electrochemical solar cell standpoint, were also observed, as might be expected for films having high electronic conductivity. For polypyrrole electrodeposited on metallic electrodes, conductivities in the 10-100 Ω^{-1} cm^{-1} range have been reported (2).

In the present paper, details of our earlier work and results obtained for other semiconductor materials are presented. Emphasis is on the stabilization provided by polypyrrole films and their effect on the photoanode performance characteristics. The role of redox couples, both in the electrolyte and incorporated within the polymer matrix, is also discussed.

Experimental Details

Unless otherwise noted, polypyrrole films were electrodeposited from mechanically stirred acetonitrile solutions containing 0.5M pyrrole and 0.2M Et_4NBF_4 (supporting electrolyte). Based on a few experiments, comparable results were obtained for films deposited from analogous methylene chloride electrolytes, and from aqueous H_2SO_4 solutions (pH 1.5-1.9) containing 0.2-0.5M pyrrole. The counterelectrode was a 25 cm^2 Pt foil. Deposition on Pt electrodes was performed at a constant potential of +0.85V *vs.* SCE (saturated calomel electrode). Deposition on n-type semiconductors was performed under tungsten-halogen illumination (100 mW/cm^2) at constant potential (0.45V *vs.* SCE for n-GaAs, 0.2V for the Cd chalcogenides, and 0.4V for n-Si) such that the current, which remained practically constant except for an initial spike, was in the 2-3 mA/cm^2 range. Based on the charge passed (20 mC/cm^2), the film thickness used in the present work was 50-100 monolayers. All electrode potentials are reported *vs.* SCE and measurements were made with *IR* compensation. Illumination for photoresponse studies was also provided by a tungsten-halogen lamp. Additional experimental details are given elsewhere (1).

Semiconductors were single crystals (~0.2 cm^2) and were polished using aqueous alumina slurries to 1 μm particle size before mounting in RTV silicone rubber (M-Coat C, M-Line Accessories, Romulus, MI). Crystal orientations were perpendicular to the c-axis for CdS and CdSe, <111> for CdTe, and <111> or <110> (comparable results) for GaAs. Ohmic contacts were made by standard techniques. GaAs electrodes were etched in a 1:1 mixture of concentrated H_2SO_4 and 30% H_2O_2 for about 15 sec (until matte black finish was obtained) prior to use. Si electrodes were etched in 49% aqueous HF solution for 10 sec. CdSe, CdTe, and CdS electrodes were etched in 4M HNO_3, concentrated HNO_3, and 6M HCl, respectively. CdSe and CdTe were dipped in a polyselenide solution after etching.

Results and Discussion

Electrodeposited polypyrrole films were first prepared (on Pt electrodes) by Diaz *et al.* (2), who also investigated their electrical and electrochemical properties (2-4). They found that films deposited from acetonitrile/tetraethylammonium tetrafluoroborate electrolytes are adherent (on metal electrodes) and consist of polymerized pyrrole units plus BF_4^- anions, typically in the ratio of about 4:1 (2). The films are stable in air to at least 250°C (3) and as electrodes in both aqueous and nonaqueous electrolytes (2-4). Reversible electrochemical oxidation of the film is evident from cyclic voltammetry and is associated with a transition from insulating (reduced form) to highly conducting (oxidized form) behavior (4). This film redox process involves exchange of anions between the film and the electrolyte, as evidenced by the dependence of the redox potential on the nature of the electrolyte (4). Anodic of the transition potential (about −0.2V *vs.* SCE in both aqueous and acetonitrile solutions), polypyrrole films exhibit electrochemical behavior similar to that observed for Pt electrodes, *i.e.*, solution redox reactions occur reversibly. Data obtained in our laboratory are in general agreement with these results, except that the films appear to slowly decompose with potential cycling in aqueous solutions (containing ferro-ferricyanide) of pH > 13, long-term stability above pH 10 being questionable.

Electroactive species can also be incorporated in the film matrix. For example, polypyrrole films containing $Fe(CN)_6^{3-}$ are produced from acetonitrile electrolytes containing this anion instead of BF_4^-. Cyclic voltammograms for a polypyrrole-$Fe(CN)_6^{3-}$ film (on Pt) in an aqueous ferro-ferricyanide solution are shown in Fig. 1. Voltammetry peaks corresponding to the $Fe(CN)_6^{3-/4-}$ redox reaction are evident at about 0.2V. The linear dependence of the peak heights on sweep rate and the near coincidence of the anodic and cathodic peak potentials are characteristic of a surface-bound redox species. The voltammetric behavior depicted in Fig. 1 was unchanged after more than 50 cycles. Upon transfer of such electrodes to solutions not containing electroactive species, the peaks corresponding to the $Fe(CN)_6^{3-/4-}$ reaction gradually disappear as the redox species is lost to the solution. Likewise, the ferro-ferricyanide reaction on polypyrrole films deposited from solutions containing only BF_4^- anions initially exhibits the reversibility characteristic of Pt (some peak separation) but the anodic and cathodic peaks become more coincidental with potential cycling in the ferro-ferricyanide solution.

* Electrochemical Society Active Member.
[1] Present address: Solar Energy Research Institute, Golden, Colorado 80401.
Key words: electrochemical solar cells, photoanode stabilization, polymer films.

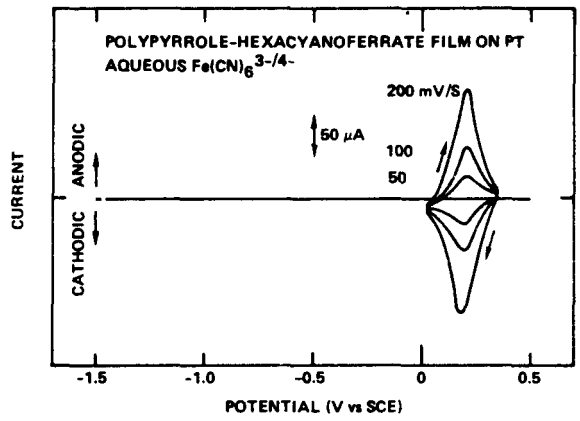

Fig. 1. Cyclic voltammograms at various sweep rates for a polypyrrole-$Fe(CN)_6^{3-}$ film on Pt (~0.1 cm^2) in aqueous 0.1M $Fe(CN)_6^{3-/4-}$ solution (pH ~10).

These results show that electroactive species can be incorporated within polypyrrole films and clearly demonstrate the mobility of anions in the polymer matrix.

Photoanode stabilization.—As discussed previously for n-GaAs (1), polypyrrole films stabilize semiconductor photoanodes against degradation while permitting electron exchange with the electrolyte. This is illustrated for n-GaAs in Fig. 2, n-CdSe in Fig. 3, and n-Si in Fig. 4. In all cases, the short-circuit photocurrent for the unprotected (bare) semiconductor decays rapidly (within a few minutes), presumably because of formation of an insoluble blocking surface layer of photodecomposition product, whereas that for the polypyrrole-coated photoanodes remains practically constant. Note that polypyrrole films also afford n-GaAs electrodes protection from dissolution in aqueous electrolytes, although in this case stabilization is less obvious since the photodecomposition products are typically soluble (5). At longer times, the film generally peels from the semiconductor surface *in toto* and the photocurrent decays. This is evident in Fig. 4 for coated n-Si after about 3 min. However, in some cases the film remains intact for several days (Fig. 2) and charge equivalent to more than the total weight of the crystal is passed without significant weight loss or degradation of the surface (inspected after film removal). Roughening the semiconductor surface by abrasion prior to film deposition appears to improve the film adhesion.

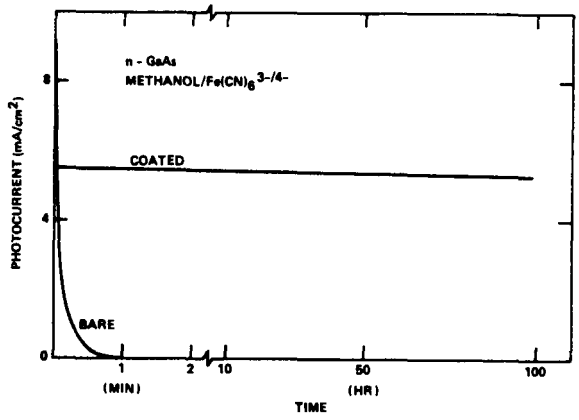

Fig. 2. Short-circuit photocurrent vs. time for bare and polypyrrole-coated n-GaAs electrodes in methanol/0.2M $Fe(CN)_6^{3-/4-}$/0.1M Et_4NBF_4 solution.

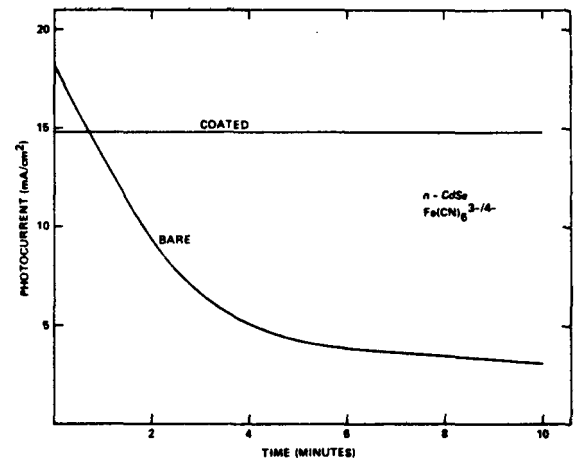

Fig. 3. Short-circuit photocurrent vs. time for bare and polypyrrole-coated n-CdSe electrodes in aqueous 0.2M $Fe(CN)_6^{4-}$/0.1M $Fe(CN)_6^{3-}$ solution (pH ~13).

Peeling problems may be associated with the permeability of polypyrrole films to solvent/solute species, since film stability appears to depend on the nature of the redox couple and/or pH of the electrolyte and in certain instances semiconductor decomposition underneath polypyrrole films is apparent. For example, polypyrrole-coated n-CdSe photoanodes are stabilized by $Fe(CN)_6^{3-/4-}$ electrolytes (pH = 10-13), but in $Fe^{3+/2+}$ perchlorate solutions (pH = 1), a red layer, presumably Se°, forms within a few minutes under the polymer film (which appears to be intact). These and related observations with a variety of semiconductor materials suggest that polypyrrole films are permeable to solvent/solute species, and that some photodecomposition may occur at the film-semiconductor interface, eventually causing the film to peel. The anion mobility discussed in the preceding section is in accord with this view. Insoluble decomposition products, *e.g.*, hydroxides, Se°, etc., may in some cases collect at the semiconductor-film interface and hinder or slow further degradation.

The apparent permeability of polypyrrole films to solvent/solute species poses a serious question regard-

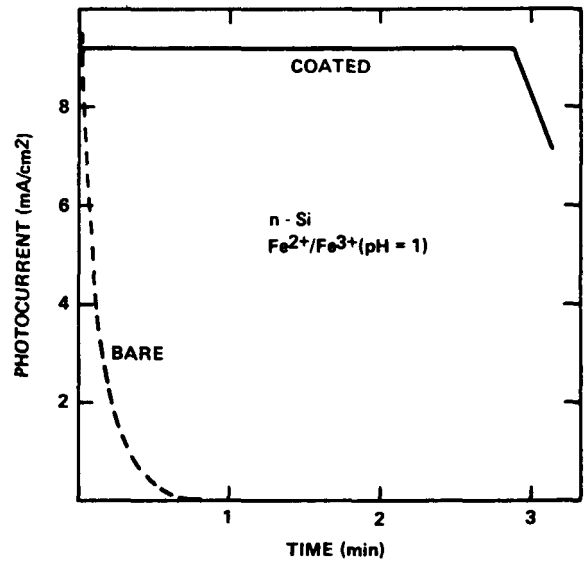

Fig. 4. Short-circuit photocurrent vs. time for bare and polypyrrole-coated n-Si in aqueous 0.2M $Fe(ClO_4)_2$/0.1M $Fe(ClO_4)_3$/0.1M $HClO_4$ solution.

ing the long-term stability of solar conversion devices employing such films. However, it may be possible to circumvent this problem. For example, sufficiently large immobile anions or redox species included in the film during electrodeposition would be expected to significantly reduce the film permeability. Encouragement for this approach is provided by the observed oxidation/reduction of the $Fe(CN)_6^{3-/4-}$ within the polypyrrole film matrix (see preceding section). Although the hexacyanoferrate species was found to be mobile in polypyrrole, there are many larger organic redox species for which this should not be the case. For example, we have deposited conducting polypyrrole films on Pt from acetonitrile/0.01M Cu(SPc)/0.1M pyrrole, where SPc is the tetrasulfophthalocyanin tetraanion. The photoelectrochemical properties of such films are currently under investigation. Other approaches are, of course, also possible, including the use of other conducting polymer films or a synergistic combination of film and electrolyte redox couple to provide long-term photoanode stability. Along these lines, we have deposited polyaniline films (6) on various semiconductors with results comparable to those obtained for polypyrrole.

Output characteristics of coated photoanodes.—Polypyrrole films apparently do not significantly affect the semiconductor energy levels important in photoelectrochemical processes. Thus, for film-coated electrodes, the flatband potential (V_{FB}) determined by a-c impedance or from the photocurrent onset, is practically unchanged, compared to the bare electrode, and remains dependent on the pH of the electrolyte. Also, except for the Cd chalcogenides and Si in acidic ferro-ferricyanide solutions, where appreciable cathodic dark currents are observed, the measured open-circuit photovoltages (V_{oc}) are generally close to the expected values ($V_R - V_{FB}$), where V_R is the electrolyte redox potential. This is illustrated by the data in Table I, for which V_{FB} values were determined from the photocurrent onset and may not correspond to those measured by a-c impedance in all cases. The V_R values, which were measured at a Pt electrode, correspond well with the standard handbook $E°$ values. Note that the V_{oc} values for polymer-coated n-GaAs and n-CdTe in ferro-ferricyanide solution containing excess CN^- are practically equivalent to the bandgap of the respective semiconductors. The increase in V_{oc} produced by excess CN^- can be accounted for by the observed negative shift in V_{FB}, but irreversible photooxidation of adsorbed CN^- (*e.g.*, to CNO^-) may also play a role. Since the cell voltage rapidly goes to zero when the electrode illumination is interrupted, the effect of the latter is probably small.

Table I. Measured and calculated open-circuit voltages (V_{oc}) for various polypyrrole-coated photoanodes in aqueous solutions

Semiconductor	Electrolyte*	V_{FB} (V vs. SCE)	Calculated V_{oc} ($V_R - V_{FB}$)	Measured V_{oc}
n-GaAs	A	−0.5	1.0	0.95
	B	−0.5	0.8	0.6
	C	−1.1	1.3	1.2
	D	−1.3	1.5	1.37
n-CdTe	A	−0.2	0.7	0.55
	B	−0.2	0.55	0.2
	C	−1.15	1.4	1.2
	D	−1.25	1.5	1.3
n-CdSe	A	−0.1	0.6	0.5
	B	−0.1	0.45	0.1
	C	−0.8	1.0	0.9
	D	−1.1	1.3	1.1
n-CdS	A	−0.4	0.9	0.65
	B	−0.4	0.75	0.3
	C	−0.8	1.0	0.9
	D	−1.3	1.5	1.25
n-Si	A	0.0	0.5	0.4

* Electrolyte A is 0.2M Fe^{3+}/0.1M Fe^{2+} perchlorates (pH = 1, V_R = 0.51V); electrolyte B is 0.2M $Fe(CN)_6^{4-}$/0.1M $Fe(CN)_6^{3-}$ (pH = 1, V_R = 0.35); electrolyte C is 0.2M $Fe(CN)_6^{4-}$/0.1M $Fe(CN)_6^{3-}$ (pH = 13, V_R = 0.22); and electrolyte D is 0.2M $Fe(CN)_6^{4-}$/0.1M $Fe(CN)_6^{3-}$/0.1M CN^- (pH = 13, V_R = 0.22V).

The effect of the polymer film on the photocurrent was difficult to ascertain since results for films produced under ostensibly the same conditions were variable, probably because of the difficulties associated with reproducing the substrate surface and film thickness. The latter was assumed to be directly proportional to the charge passed during deposition which may not be a valid assumption, especially since some semiconductor photodegradation undoubtedly occurs as deposition is initiated. In some cases, the photocurrents for the polymer-coated electrodes approached those for the bare semiconductor but the behavior depicted in Fig. 5 was more typical. In this case, the film is seen to reduce the photocurrent by about 30%. This reduction could be due to light absorption within the film or enhanced charge carrier recombination associated with interface states formed at the semiconductor-film interface. As mentioned previously, the reduction in open-circuit voltage (Fig. 5) is apparently due to cathodic dark current introduced by the film, which suggests that interface states may play a role. However, if such effects are not too pronounced, performance characteristics for polypyrrole-coated electrodes could approach those for the bare semiconductor for sufficiently thin films. Of course, a compromise would be required between photoanode stability and performance.

Summary and Conclusions

The results presented here show that electrodeposited polypyrrole films suppress photodegradation of semiconductor photoanodes while permitting efficient electron exchange with the electrolyte. Performance characteristics attainable with such film-coated photoanodes are typically comparable to those obtained for the bare electrode. Peeling is currently a problem which appears to be associated with permeability of the film to solvent/solute species. One promising approach for future work is to incorporate immobile redox species

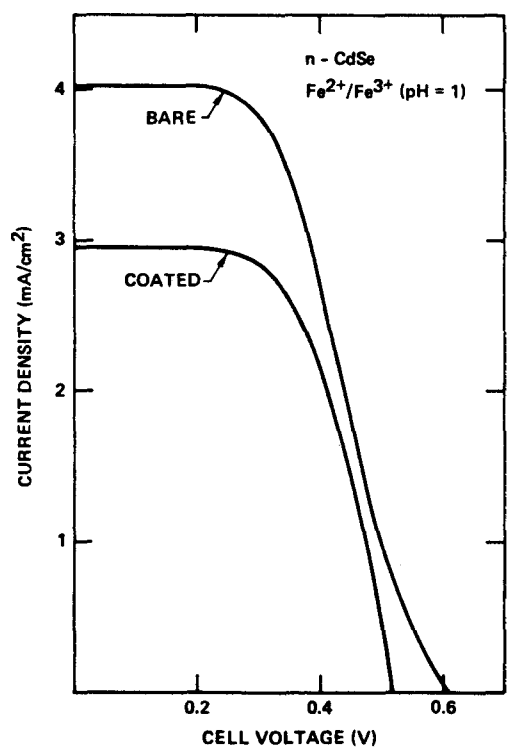

Fig. 5. Photocurrent-voltage curve for bare and polypyrrole-coated n-CdSe in aqueous 0.2M $Fe(ClO_4)_2$/0.05M $Fe(ClO_4)_3$/0.1M $HClO_4$ solution.

in the film to reduce permeability to electrolyte solvent/solute species.

Acknowledgment

The authors gratefully acknowledge support of this work by the Solar Energy Research Institute under Subcontract No. XG-0-9276.

Manuscript submitted March 16, 1981; revised manuscript received June 22, 1981.

Any discussion of this paper will appear in a Discussion Section to be published in the June 1982 JOURNAL. All discussions for the June 1982 Discussion Section should be submitted by Feb. 1, 1982.

Publication costs of this article were assisted by Rockwell International.

REFERENCES

1. R. Noufi, D. Tench, and L. F. Warren, *This Journal*, **127**, 2310 (1980).
2. A. F. Diaz, K. K. Kanazawa, and G. P. Gardini, *J. Chem. Soc. Chem. Commun.*, 635 (1979).
3. K. K. Kanazawa, A. F. Diaz, R. H. Geiss, W. D. Gill, J. F. Kwak, J. A. Logan, J. F. Rabolt, and G. B. Street, *ibid.*, 854 (1979).
4. A. F. Diaz and J. I. Castillo, *ibid.*, 397 (1980).
5. H. Gerischer, *Ber. Bunsenges.*, **69**, 578 (1965).
6. A. F. Diaz and J. A. Logan, *J. Electroanal. Chem. Interfacial Electrochem.*, **111**, 111 (1980).

Reprinted from JOURNAL OF THE ELECTROCHEMICAL SOCIETY
Vol. 128, No. 12, December 1981
Printed in U.S.A.

APPENDIX II

Extended abstract of a paper on electrogenerated polyaniline films presented at the Denver Electrochemical Society Meeting, Oct. 11-16, 1981.

ENHANCED STABILITY OF PHOTOELECTRODES WITH ELECTROGENERATED POLYANILINE FILMS

Rommel Noufi and Arthur J. Nozik
Solar Energy Research Institute, 1617 Cole Blvd.
Golden, Colorado 80401

John White and Les F. Warren
Rockwell International/MRDC
1049 Camino Dos Rios, Thousand Oaks, California 91360

ABSTRACT

Polyaniline was electrodeposited on platinum and semiconducting (Cd-chalcogenides, Si, GaAs, GaP) electrodes from aqueous solution (pH = 1) containing aniline. The electrochemical behavior of such films was examined in aqueous and nonaqueous solutions by cyclic voltametry. Results show that the polyaniline film is conducting in both cathodic and anodic regions at pH $<$ 3 as evidenced by the electrochemical redox reactions of various redox couples on polyaniline-coated electrodes. In general, all polyaniline-coated semiconductor electrodes examined in this work exhibited enhanced stability of the photocurrent when compared to that of the naked electrodes.

INTRODUCTION

Coating electrode surfaces with polymers has been used to stabilize the substrate against corrosion (1). The electrodeposition of conducting polypyrrole films on the surface of semiconductor photoanodes has been recently shown to decrease photocorrosion (2-6). This film, acting as a barrier to ion/solvent transport, inhibits photodegradation of the electrode surface while permitting electron exchange with the electrolyte. Hence, one can utilize redox reactions, otherwise not applicable, to yield maximum open-circuit photovoltage (2), to improve stability (3), and to promote high conversion efficiency of light into electricity or chemical fuels (e.g., H_2). Furthermore, by incorporating catalysts or sensitizers into the polymer films, we can increase the rate of certain reactions.

In addition to studies of polypyrole films on semiconductor electrodes, the properties of polypyrrole films deposited on metal electrodes have also been investigated (7-9). In this paper, we describe the electrochemical properties of polyaniline coated onto Pt electrodes and various n- and p-type photoelectrodes. Deposition of polyaniline on Pt electrodes has recently been reported (10). Unlike polypyrrole, polyaniline films are electronic conductors in both the cathodic and anodic potential regions (10); thus both oxidation and reduction reactions can be carried out on polymer-coated electrodes.

EXPERIMENTAL

Polyaniline films were electrodeposited by the oxidation of aniline from quiet aqueous solutions containing 1 M aniline and 0.05 M Na_2SO_4 at pH = 1. The electrodeposition on Pt was carried out either potentiostatically at +0.9 V or by sweeping the electrode potential between -0.2 and +0.9 V. The deposition on semiconductor electrodes was carried out potentiostatically at potentials between 0 and +0.4 V for n-type materials, and between +0.4 and 1.2 V in the dark for p-type materials, both under tungsten halogen illumination (100 mW/cm^2).

Film thickness was monitored by measuring the charge passed. A charge of 24 mC/cm^2 yielded a film thickness of about 0.1 μm as extrapolated from Reference 7. Illumination for photoresponse studies was provided by a tungsten-halogen lamp.

Semiconductor electrodes were single crystals (except n-Si) and were polished using 0.3 μm alumina slurries. The n-type Si was polycrystalline (20Ω-cm) material with grain size about 1.5 x 4 mm. The p-type Si was single crystal (1Ω-cm). Crystal orientations were $\langle 11\bar{2}0 \rangle$ for n-CdSe, $\langle 111 \rangle$ or $\langle 110 \rangle$ (comparable results) for p-GaAs, and $\langle 100 \rangle$ for p-GaP. Ohmic contacts were made by standard techniques. Si electrodes were etched in 49% aqueous HF solution for 10 seconds, CdSe was etched in 5 M HNO_3 for 10 seconds, GaAs in concentrated H_2SO_4 and 30% H_2O_2 for about 15 seconds, and GaP in 1:1:3 H_2O + 30% H_2O_2 + concentrated H_2SO_4 at about 80°C for 5 seconds. Additional experimental details are given elsewhere (2).

Results and Discussion

Film Electroactivity — Reversible electrochemical oxidation of the polyaniline film in 0.1 M Na_2SO_4 (pH=1) is evident from cyclic voltammetry (Figure 1), and is associated with a proton addition (reduced form)/proton elimination (oxidized form) reaction (11). The voltammogram is complex but shows well defined electroactive regions. The anodic and cathodic current peaks change linearly with scan rate as expected from surface-attached species, except for the most positive reduction peak which exhibited changes in peak height and position depending on the switching potential at the more positive end of the potential scale. Switching at more positive potentials produced a higher peak which shifted to less positive potentials.

The film also exhibits electroactivity in acetonitrile solutions as was observed by Diaz and Logan (10). On the other hand, electroactivity is absent in methanol and ethanol, and also when the pH of the aqueous solutions is greater than ca. 3.

Electrochemistry of solution redox species — Polyaniline on Pt is conducting in both the anodic and cathodic regions. The oxidation and reduction of several redox species in aqueous and acetonitrile solutions were driven in the potential range between +1 and -1V. Figure 2 shows a cyclic voltammogram of the redox reaction of $Fe^{2+/3+}$ in 0.1 M Na_2SO_4 (pH = 1). The redox peaks of $Fe^{2+/3+}$ appear superimposed on the background electroactivity of the film and are centered around +0.42 V, which is the equilibrium potential of $Fe^{2+/3+}$ measured in the same solution with a naked Pt electrode. However, when the peak separation ΔEp for the redox reaction of $Fe^{2+/3+}$ with polyaniline-coated electrodes (Pt/PA) is compared with naked Pt, one observes a dramatic enhancement of the reversibility of the reaction at Pt/PA (Figure 3). This enhancement in the kinetics (i.e., electrocatalysis) of the reaction was also observed on other electrodes (e.g., carbon and tantalum). The electrocatalytic properties of polyaniline on metallic and carbon electrodes is discussed elsewhere (12).

Figure 4 shows the electrochemistry of $Fe(CN)_6^{3-/4-}$ in aqueous solution (pH = 1) at a Pt/PA electrode compared to a naked Pt electrode. Both voltammograms are centered around the equilibrium potential for $Fe(CN)_6^{3-/4-}$ in the H_2SO_4 electrolyte. The reaction on Pt is disfusion control, and the peak currents have a square root dependence on scan rate. The reaction on Pt/PA is that of a surface-bound species, as evidenced by the shape of the waves; however, the peaks do not coincide nor do their heights scale linearly or as the square root with scan rate. This suggests a diffusional contribution by the species through the film (13). The redox reaction of $Fe(CN)_6^{3-/4-}$ in acetonitrile was also driven at potentials similar to that on naked Pt (-0.75V) with wave characteristics similar to the reaction in water but with broadening of the peaks.

Stabilization of Photoelectrodes — The stability of the photocurrent of n- and p-type polyaniline-coated electrodes was examined for reactions involving reversible solution species and H^+ reduction. Figure 5 shows the dramatic enhancement in the photocurrent stability of the n-Si/PA photoanode compared to the naked electrode. The gradual decrease observed after 50 hours is accompanied by wrinkles in the film suggesting undermining of the film by the liquid. Similar stability was demonstrated for a p-Si/PA photocathode for the reduction of $Fe(CN)_6^{4-}$ (Eq = -0.75 V in acetonitrile). Figure 6 compares the current-potential curves for a coated and a naked p-Si electrode. Note the enhancement in the cathodic photocurrent and anodic dark current for the coated electrode. In this experiment the cathodic currents are limited by the bulk concentration of the $Fe(CN)_6^{4-}$ and not by light intensity. The enhancement in the photoreduction current is also evident for the reduction of H^+ (Figure 7); note also the increase in the dark reduction current in this case.

Hydrogen ion reduction on p-GaP/PA is similar to that on the p-Si/PA with respect to photocurrent enhancement. The behavior of the photoreduction with time is compared with the naked p-GaP (Figure 8). The photocurrent at p-GaP starts (t = o) higher than for the case of p-GaP/PA, and then decays at a faster rate until it reaches a steady state.

The stability of n-CdSe and p-GaAs in aqueous and nonaqueous solutions are also enhanced when coated with polyaniline. Figures 9 and 10 show current-potential curves and current-time behavior of the coated and naked electrodes. The n-CdSe photoanodes show an initial increase for a few minutes, then a gradual decay of the photocurrent with time, and show a visual roughening of the surface, with some buildup of a reddish Se layer after 2 hours. The photocurrent of the coated electrodes decayed initially by about 10% in the first few minutes, but stayed at a higher current compared to the naked electrode after 2 hours. No visual buildup of Se was observed. With p-GaAs in acetonitrile solution, the enhancement in photocurrent and stability is more dramatic as shown in Figure 10.

The polyaniline film apparently does not significantly affect the semiconductor energy levels. Thus, for film-coated electrodes, the onset of the photocurrent is practically unchanged compared to the naked electrode. The measured open-circuit photovoltages were generally close to the expected values of $(V_r - V_{fb})$, where V_r is the electrolyte equilibrium potential and V_{fb} is the flat band potential for the naked electrodes, as reported in the literature and determined in this work from the onset of the photocurrent. The same observation was also reported for polypyrrole-coated electrodes (6).

The increased stability can be attributed to the rapid removal of photogenerated charge from the electrode surface before it can react with the electrode material. The kinetics of the photocharge transfer to solution species, mediated by the film, become favorable compared to the reaction with the semiconductor lattice material or to recombination.

Figure 11 is a schematic of a possible mechanism for the charge transfer for both coated and uncoated electrodes (an n-type electrode is used for illustration). In the case of the naked electrode (Figure 11a), decomposition is favored when Reaction [1] is faster than reaction [2]. The situation for film-coated electrodes is shown in Figure 11b. In an ideal situation in which the conducting film is pinhole free and unpermeable, only Reaction [4] will occur since there is no contact between the semiconductor and the solution (for simplicity we neglect electron-hole recombination). However, since pinholes and permeability are most likely present, Reaction [3] is also possible, and is depicted here at a micropore. Because the film is conducting and enhances the charge transfer to the solution species, it channels photogenerated charge away from the micro-pore. Thus there is enhancement in the rate of Reaction [4] over the other three reactions shown for the coated and naked surface. This situation then favors stabilization.

Conclusion

The results show that electrodeposited polyaniline films enhance stability of semiconductor photoelectrodes by permitting efficient charge exchange with the electrolyte. Integrity of the film is currently a problem which could be due to the permeability of the film or to less than perfect adhesion. Future work will focus on improvement in the integrity of the film deposited on semiconductor electrodes and on better understanding of the charge transfer mechanisms.

REFERENCES

1. M.S. Wrigton, R.G. Austin, A.B. Bocarsly, J.M. Bolts, O. Haas, K.O. Legg, L. Nadjo and M.C. Palaggoto, J. Am. Chem. Soc., 100, 1602 (1978).

2. R. Noufi, D. Tench, and L.F. Warren, J. Electrochem. Soc., 127, 2310 (1980).

3. R. Noufi, A.J. Frank, and A.J. Nozik, J. Am. Chem. Soc., 103, 1849 (1981).

4. F.-R.F. Fan, B.L. Wheeler, A.J. Bard, and R. Noufi, J. Electrochem Soc., 128, 2042 (1981).

5. T. Skotheim, I. Lundstrom, and J. Prajza, J. Electrochem. Soc., 128, 1625 (1981).

6. R. Noufi, O. Tench and L.F. Warren, J. Electrochem. Soc., 128, 2596 (1981).

7. A.F. Diaz and J. Castillo, J.C.S. Chem. Comm., 347, (1980).

8. R.A. Bull, F.-R.F. Fan, and A.J. Bard, J. Electrochem. Soc., submitted.

9. G. Cooper, R. Noufi, A.J. Frank, and A.J. Nozik, Nature, submitted.

10. A.F. Diaz and J.A. Logan, J. Electroanal. Chem.,111 111 (1980).

11. D.M. Mohilner, R. N. Adams, and W.J. Argersinger, Jr., J. Am. Chem. Soc., 84, 3618 (1969).

12. R. Noufi, J. Turner, and A.J. Nozik, J. Electroanal. Chem., manuscript in preparation.

13. J. Facci and R.W. Murray, J. Electroanal. Chem., 124, 339 (1981).

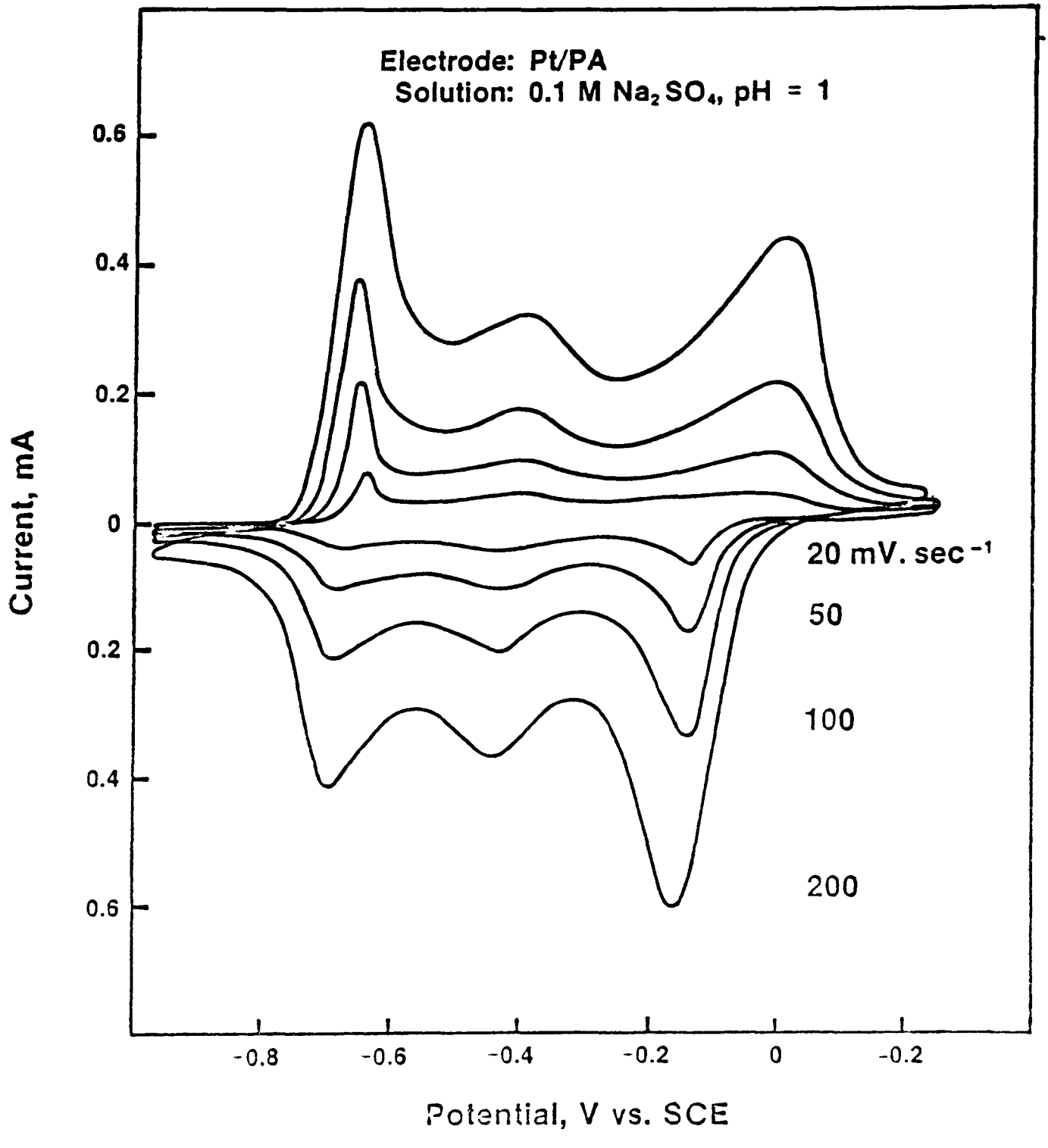
Electrode: Pt/PA
Solution: 0.1 M Na_2SO_4, pH = 1
0.6
0.4
0.2
0
0.2
0.4
0.6
Current, mA
20 mV. sec^{-1}
50
100
200
-0.8
-0.6
-0.4
-0.2
0
-0.2
Potential, V vs. SCE

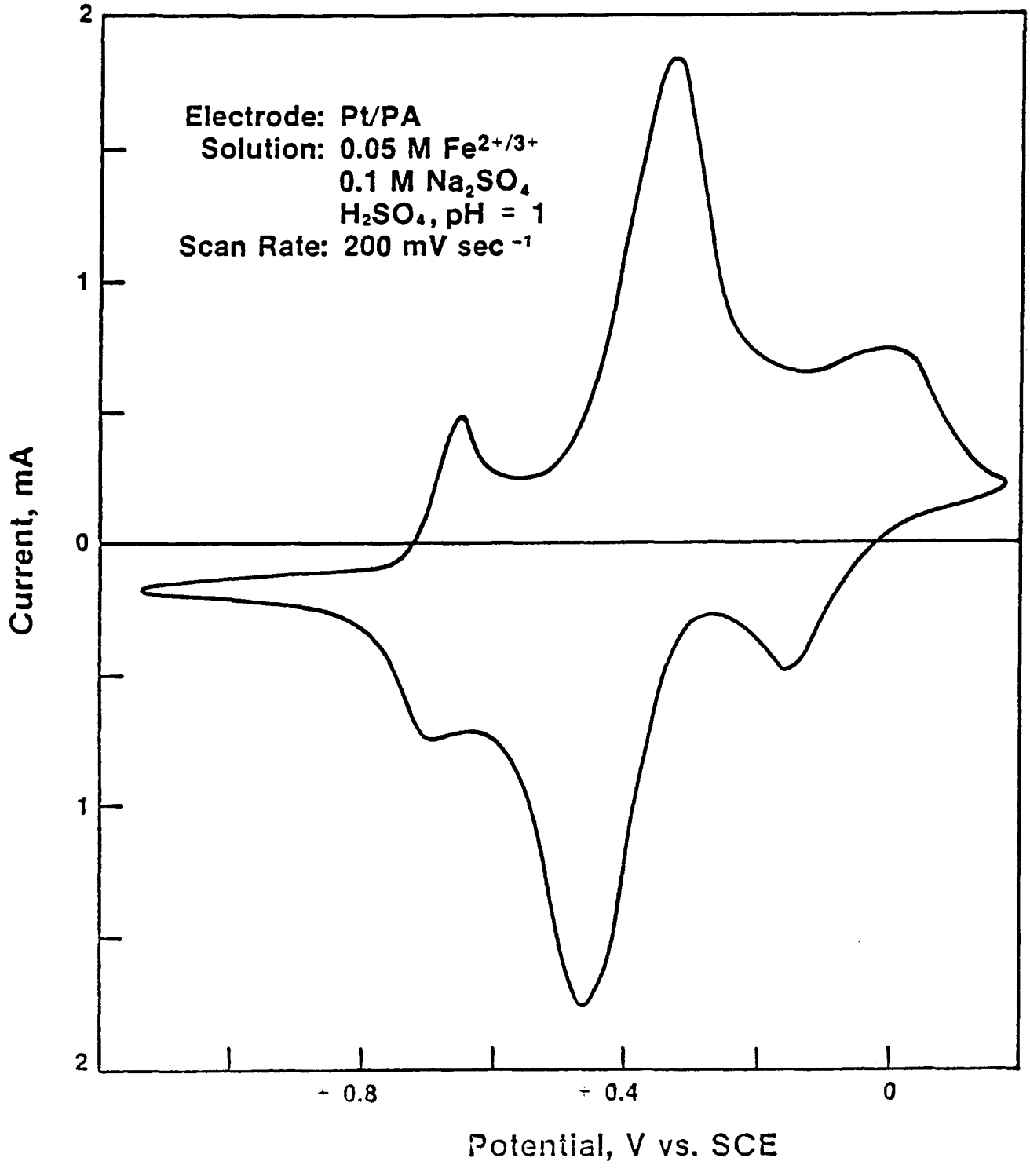
Electrode: Pt/PA
Solution: 0.05 M $Fe^{2+/3+}$
0.1 M Na_2SO_4
H_2SO_4, pH = 1
Scan Rate: 200 mV sec^{-1}
2
1
0
1
2
Current, mA
+ 0.8
+ 0.4
0
Potential, V vs. SCE

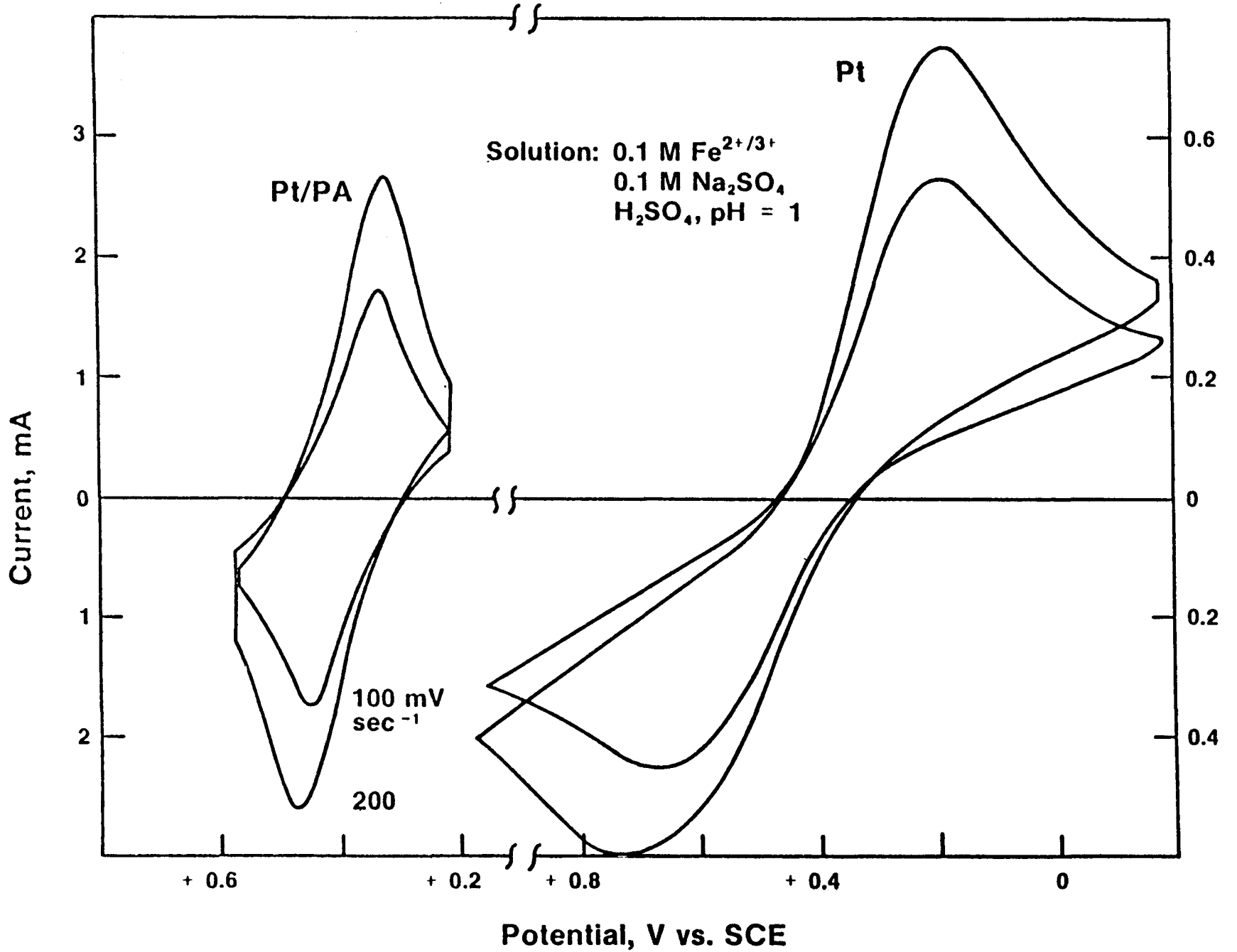
Pt
Pt/PA
Solution: 0.1 M $Fe^{2+/3+}$
0.1 M Na_2SO_4
H_2SO_4, pH = 1
100 mV
sec $^{-1}$
200
Current, mA
Potential, V vs. SCE
3
2
1
0
1
2
0.6
0.4
0.2
0
0.2
0.4
+ 0.6
+ 0.2
+ 0.8
+ 0.4
0

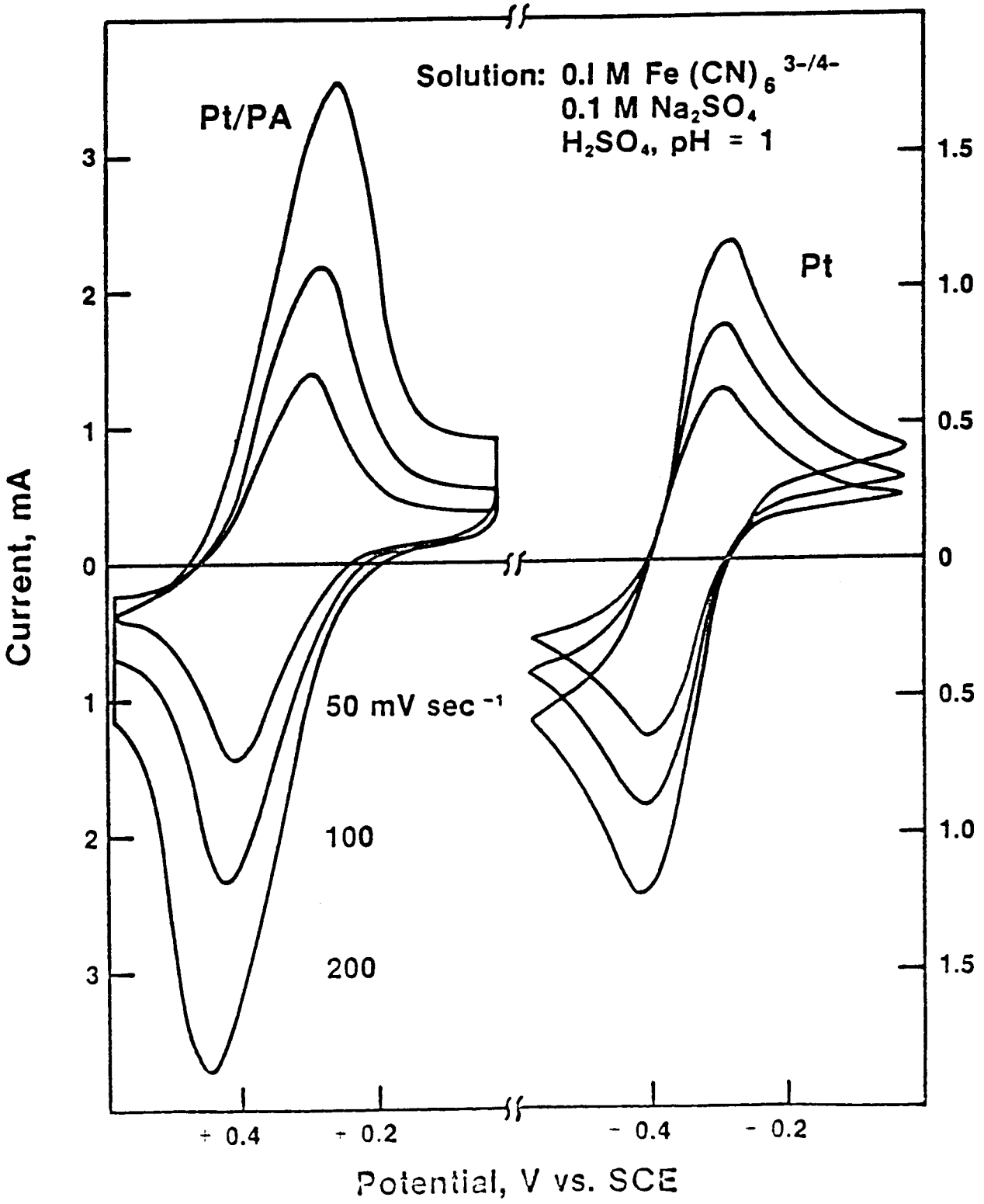
Solution: 0.I M Fe (CN) 6 3-/4-
0.1 M Na2SO4
H2SO4, pH = 1
Pt/PA
Pt
50 mV sec -1
100
200
Current, mA
Potential, V vs. SCE
+ 0.4
+ 0.2
- 0.4
- 0.2
3
2
1
0
1
2
3
1.5
1.0
0.5
0
0.5
1.0
1.5

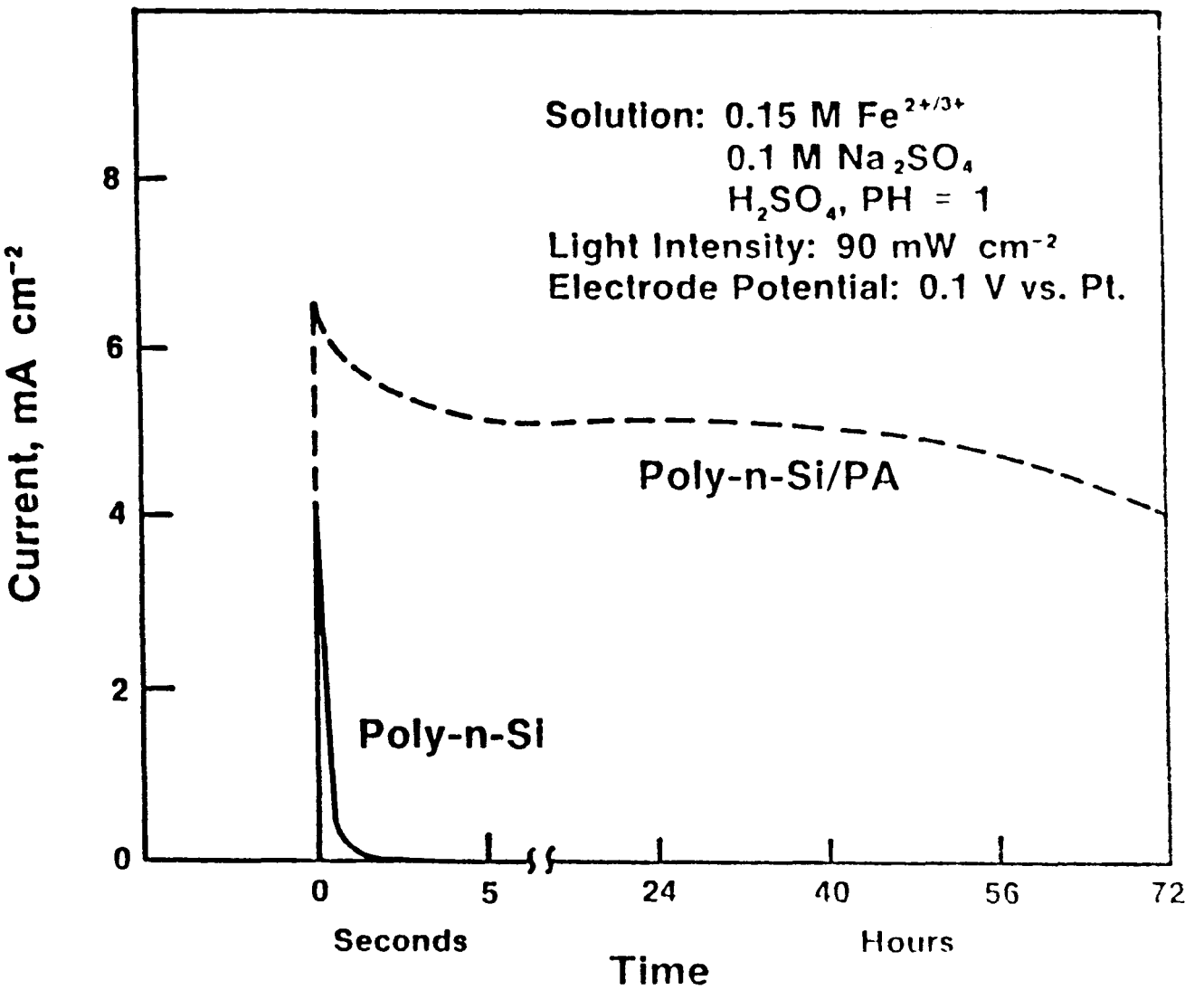
Solution: 0.15 M $Fe^{2+/3+}$
0.1 M Na_2SO_4
H_2SO_4, PH = 1
Light Intensity: 90 mW cm^{-2}
Electrode Potential: 0.1 V vs. Pt.
Poly-n-Si/PA
Poly-n-Si
Current, mA cm^{-2}
0
2
4
6
8
0
5
24
40
56
72
Seconds
Hours
Time

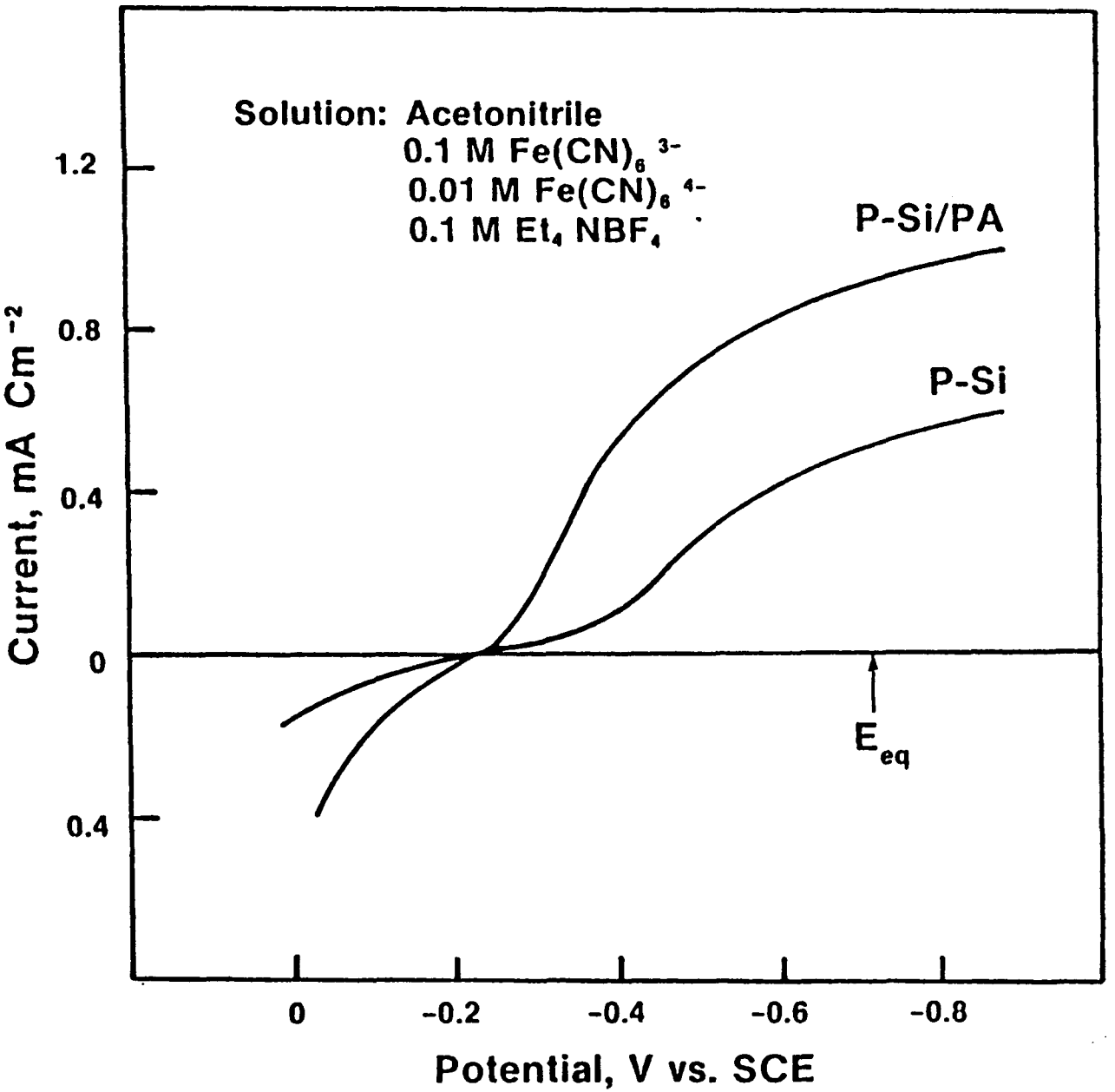
Solution: Acetonitrile
0.1 M Fe(CN)6 3-
0.01 M Fe(CN)6 4-
0.1 M Et4 NBF4
P-Si/PA
P-Si
Eeq
Current, mA Cm -2
1.2
0.8
0.4
0
0.4
0
-0.2
-0.4
-0.6
-0.8
Potential, V vs. SCE

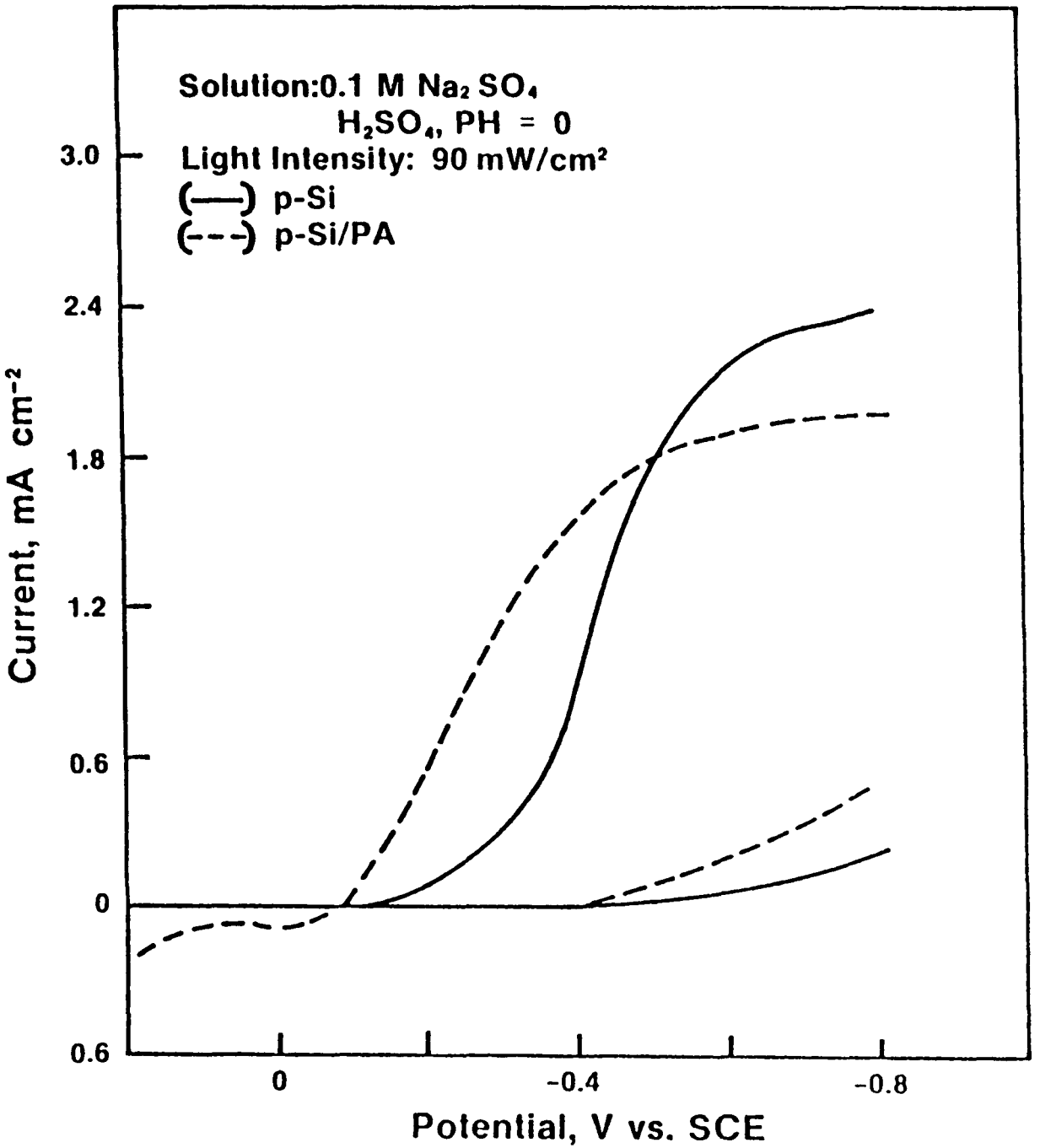
Solution:0.1 M Na_2SO_4
H_2SO_4, PH = 0
Light Intensity: 90 mW/cm²
(——) p-Si
(- - -) p-Si/PA
3.0
2.4
1.8
1.2
0.6
0
0.6
Current, mA cm⁻²
0
-0.4
-0.8
Potential, V vs. SCE

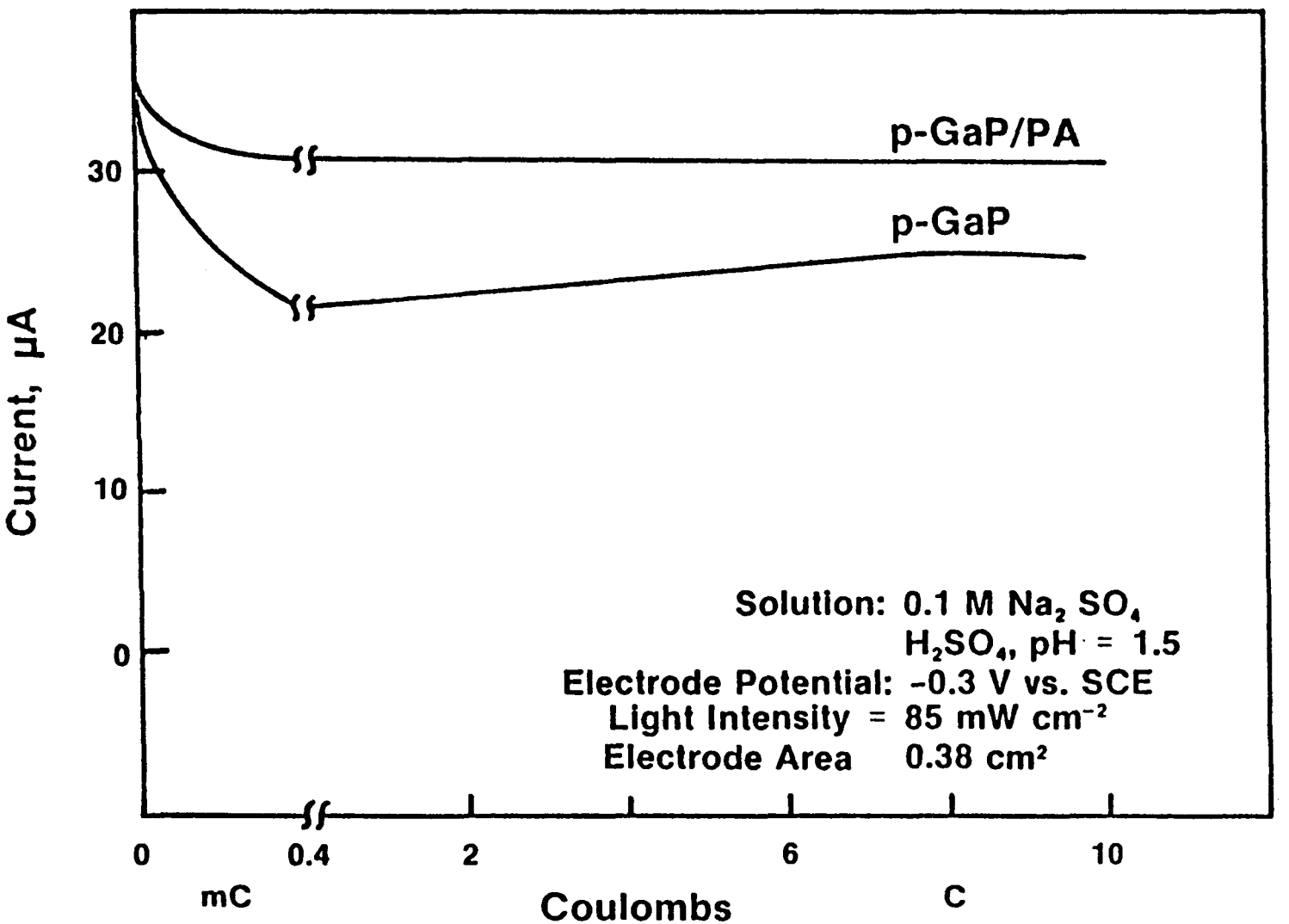
p-GaP/PA
p-GaP
30
20
10
0
Current, μA
Solution: 0.1 M Na2 SO4
H2SO4, pH = 1.5
Electrode Potential: -0.3 V vs. SCE
Light Intensity = 85 mW cm-2
Electrode Area 0.38 cm2
0
0.4
2
6
10
mC
Coulombs
C

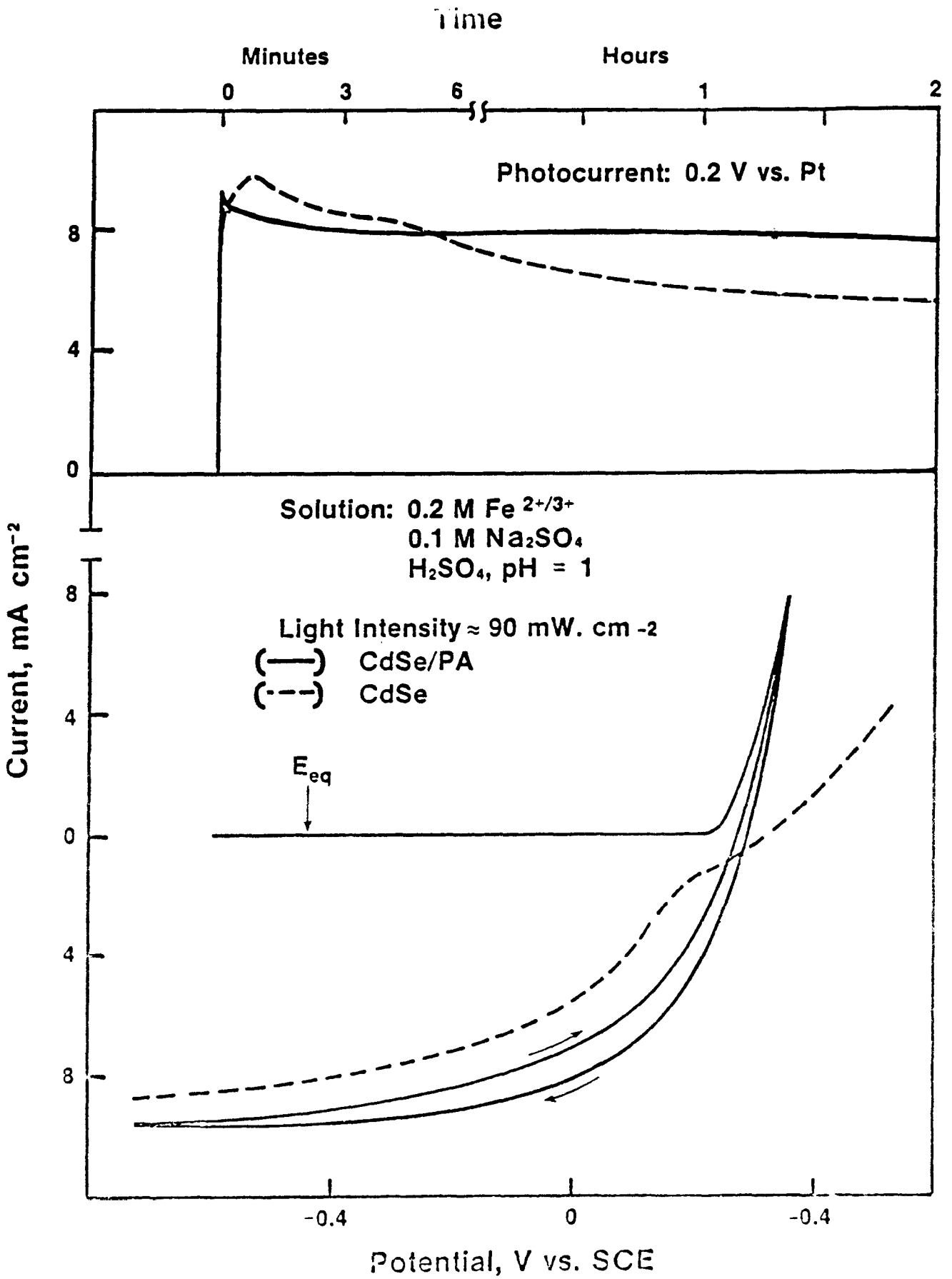
Time
Minutes
Hours
0
3
6
1
2
Photocurrent: 0.2 V vs. Pt
8
4
0
Solution: 0.2 M Fe 2+/3+
0.1 M Na2SO4
H2SO4, pH = 1
Light Intensity ≈ 90 mW. cm -2
CdSe/PA
CdSe
Eeq
Current, mA cm-2
8
4
0
4
8
-0.4
0
-0.4
Potential, V vs. SCE

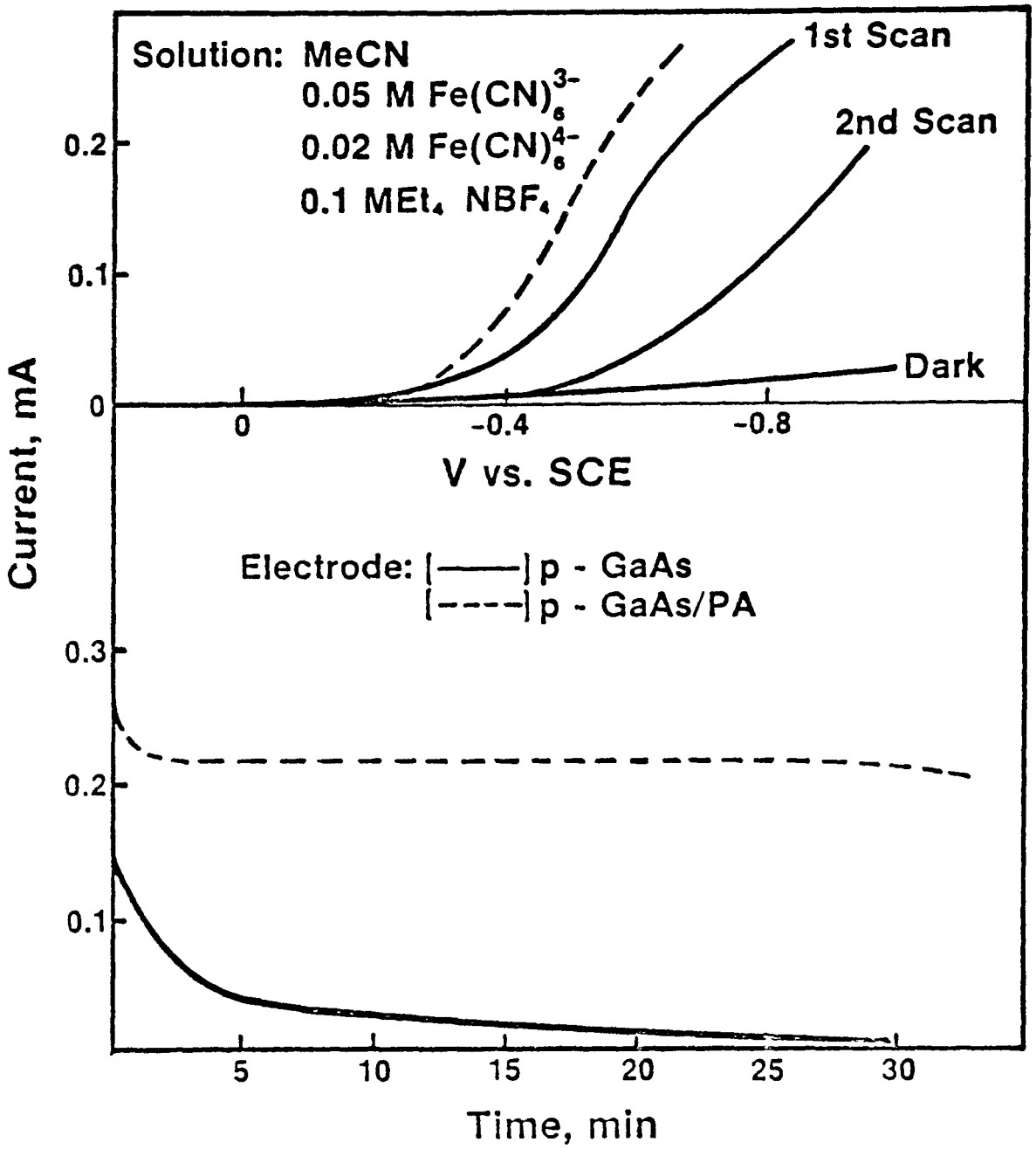
Solution: MeCN
0.05 M Fe(CN)$_6^{3-}$
0.02 M Fe(CN)$_6^{4-}$
0.1 MEt$_4$ NBF$_4$
1st Scan
2nd Scan
Dark
0.2
0.1
0
0
-0.4
-0.8
V vs. SCE
Electrode: [——] p - GaAs
[----] p - GaAs/PA
Current, mA
0.3
0.2
0.1
5
10
15
20
25
30
Time, min

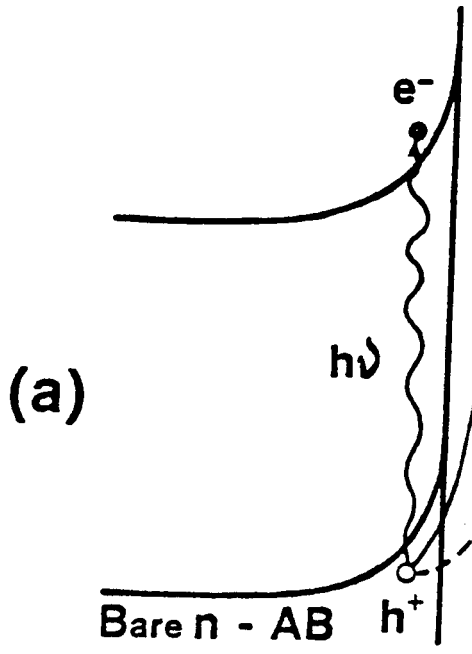

(a)

$AB + h^+ \xrightarrow[k_1]{} A^+ + B$ [1]

$R + h^+ \xrightarrow[k_2]{} O$ [2]

$k_1 > k_2$ Favors Decomposition

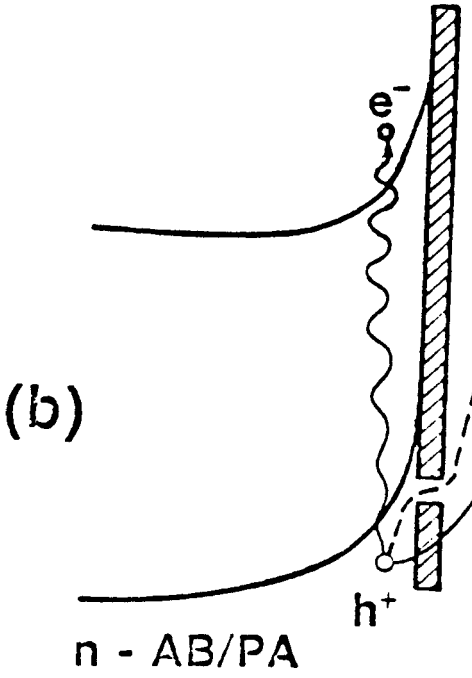

(b)

$AB + h^+ \xrightarrow[k_3]{} A^+ + B$ [3]

$R + h^+ \xrightarrow[k_4]{} O$ [4]

$k_1 > k_3$

$k_4 > k_2$ and $> k_3$ stabilizing

APPENDIX III

Paper on electrodeposited metal oxide films presented at the Montreal Electrochemical Society meeting, May 1982, and submitted to the Journal of the Electrochemical Society.

ELECTRODEPOSITION OF CONDUCTING TRANSITION METAL OXIDE FILMS FROM AQUEOUS SOLUTION

Dennis Tench and Leslie F. Warren
Rockwell International
Microelectronics Research and Development Center
Thousand Oaks, CA 91360

Key Words: metal oxides, electrodeposition procedures, electrochemical properties

Metal oxide films formed by electrochemical or chemical growth on the corresponding metal electrode have been investigated extensively. Many of these oxides are of considerable practical interest because of their charge storage capabilities (Ni, Mn), electrochromic activity (Ni, Rh, Ir), electrocatalytic properties (Ru), and photoelectrochemical activity (Cu, Ni, Fe). A simple method for the controlled application of such films onto substrates other than the metals themselves (e.g., onto semiconductors) does not appear to have been developed. We report here our preliminary results describing a general technique for the electrochemical deposition of oxide/hydroxide films of copper, nickel, cobalt, iron, and manganese from aqueous solution. The general properties of these materials, some of which are new, are also discussed.

Films were typically deposited on a 0.5 cm^2 rotating platinum disk electrode (400 rpm), either by voltage cycling (50 mV/sec) or at constant electrode potential from buffered solutions (pH 6.5 - 7.5). A sodium acetate buffer was used since, at the metal ion concentrations employed (0.10 to 0.25 M), other common buffering agents either precipitate the metal hydroxide or strongly complex the metal ion (increase the overpotential for deposition). All potentials are given relative to the saturated calomel electrode (SCE).

Figure 1 shows voltammograms associated with nickel oxide deposition. On the first anodic sweep (dashed line), only a slowly increasing anodic current is evident. On each subsequent cycle, beginning at the positive limit, corresponding reduction and oxidation peaks, for which the associated (equivalent) charge increases with each cycle, were observed. The cathodic/anodic peaks

correspond to reduction/oxidation of the nickel oxide film, which is deposited by oxidation of Ni^{2+} to Ni^{3+} and precipitates on the electrode surface, presumably as NiO(OH). Although the equations are not balanced, the overall reaction can be schematically represented as:

$$Ni^{2+} \xrightarrow{-e^-} Ni^{3+} \xrightarrow{OH^-} NiO(OH) \underset{-e^-}{\overset{+e^-}{\rightleftharpoons}} Ni(OH)_2 \qquad (1)$$

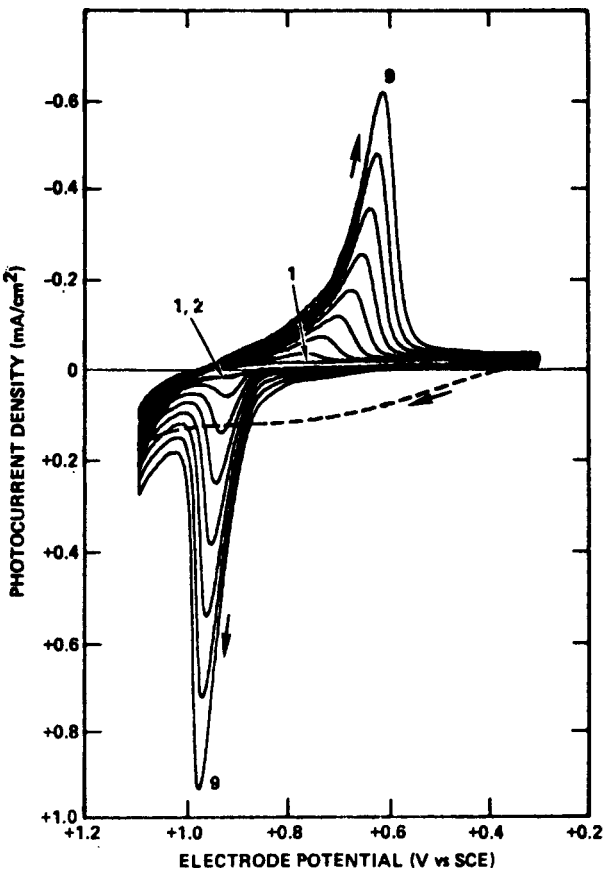

Fig. 1 Cyclic voltammograms (50 mV/sec) for a rotating Pt disk electrode (400 rpm) in an aqueous solution containing 0.13 M $NiSO_4$, 0.1 M Na_2SO_4 and 0.13 M sodium acetate (pH 7.1).

Nickel oxide films prepared by this potential cycling technique appear to be uniform and smooth, are electrically conducting, and exhibit electrochromic properties, rapidly turning from transparent to dark brown at well-defined potentials. Figure 2 shows a linear plot of film thickness, measured by ellipsometry, vs the integrated peak charge. Approximate calculations of the film thickness based on the voltammetry peak charge (Fig. 1), assuming a cubic lattice and Ni-O bond distance of 4.2 , gave comparable numbers to those derived from the ellipsometry measurements. Electrochemically, the electrodeposited films resemble the thick anodic hydrous oxide films grown on nickel electrodes in neutral or basic electrolytes [1], rather than the passive film [2]. Films having similar properties have been prepared by cathodic deposition from aqueous nickel nitrate solutions [3-5], where nitrate reduction to form hydroxide seems to be involved.

The good electrical conductivity of the nickel oxide films prepared by anodic electrodeposition is evident from the voltammograms in Fig. 3. Note that, in this basic electrolyte, the redox properties of the film, as reflected in the general shape of the voltammograms, changes somewhat with potential cycling [4]. The current waves corresponding to ferri-ferrocyanide reduction/oxidation on the oxide-covered electrode in this system (onset at 0.1 V) is virtually identical to those observed for the bare platinum electrode.

Other oxides prepared by electrodeposition from acetate-buffered solutions and the deposition conditions are listed in Table I. At a potential of 1.1 V, manganese oxide can also be deposited from acidic electrolytes (0.2 M H_2SO_4). It should be noted that manganese oxide for use in dry batteries has been prepared by anodic deposition for some time [6,7], but the deposition potential at higher pH with the acetate buffer is considerably lower. Passivating iron oxide films prepared anodically from Fe^{2+} solutions have also been described previously [8]. Film thicknesses reported below were derived from calculations similar to that used for nickel oxide films.

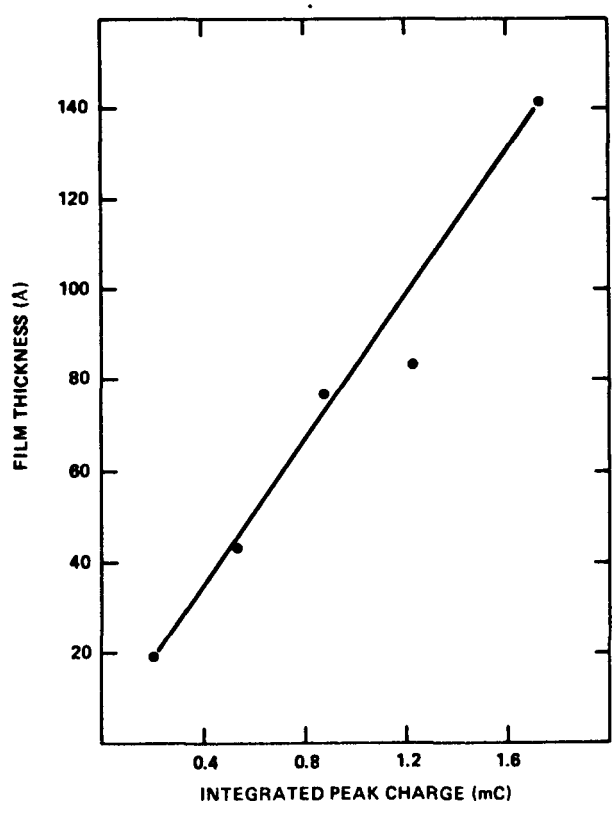

Fig. 2 Plot of the thickness of electrodeposited nickel oxide films measured by ellipsometry vs the integrated peak area (from Fig. 1).

Copper oxide films deposited cathodically at constant potential under the conditions given in Table I are orange and can be grown to a nominal thickness of about 5000Å; above this limit, the deposition current rapidly decays. The deposition process probably involves reduction of Cu^{2+} in solution and dehydration of the deposited oxide, which can be represented schematically as:

$$Cu^{2+} \xrightarrow[OH^-]{+e^-} CuOH \xrightarrow{-H_2O} Cu_2O \qquad (2)$$

Consistent with other work [9], these films were found to undergo oxidation/reduction and to gradually dissolve during potential cycling in aqueous

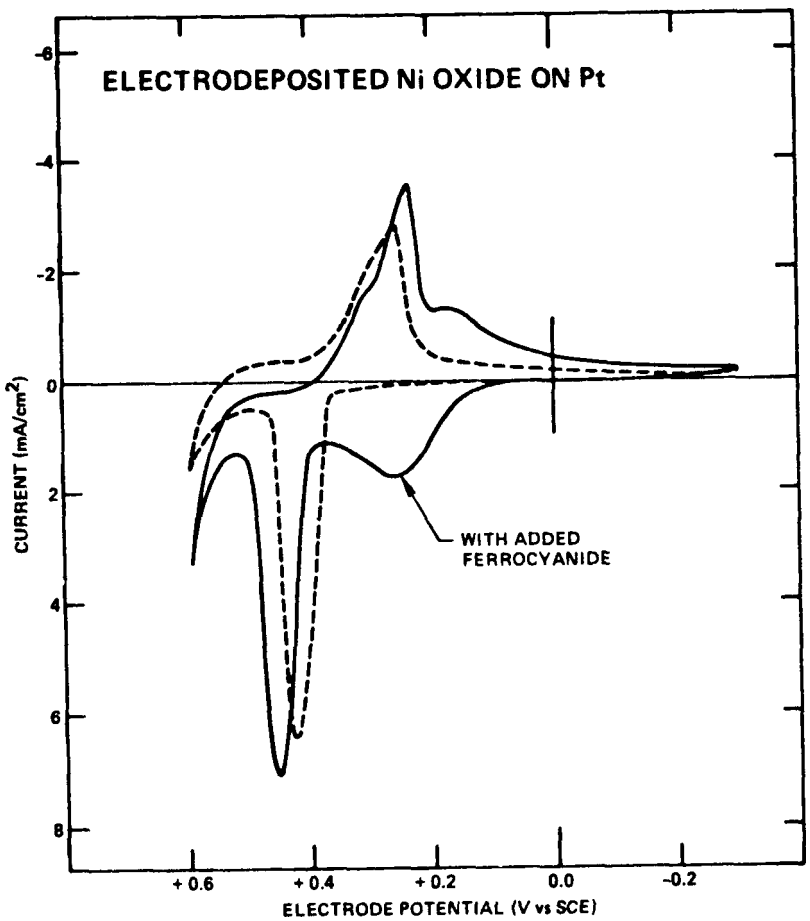

Fig. 3 Cyclic voltammograms at 50 mV/sec for a stationary electrodeposited nickel oxide film (100A) on Pt in 0.1 M NaOH, with (solid curve) and without (dashed curve) added ferrocyanide (0.01 M).

solutions. However, electrodeposited copper oxide films appear to be stable in acetonitrile electrolytes, where oxidation/reduction of the film itself is not observed, but the ferrocene/ferricenium redox reaction (E° = +0.4 V) occurs reversibly on the film-covered electrode.

Table I

Deposition Conditions for Metal Oxide Films

Metal	Solution Composition	pH	Electrodeposition Conditions	Probable Film Composition
Ni	0.13 M $NiSO_4 \cdot 6H_2O$ 0.13 M NaOAc 0.10 M Na_2SO_4	7.14	Potential cycled between +0.3 and +1.1 V at 50 mV/sec; anodic deposition	$Ni(OH)_2/NiO(OH)$
Cu	0.1 M $Cu(OAc)_2.2H_2O$ 0.8 M NaOAc (nitrogen saturated)	6.45	Constant potential at 0.0 V; cathodic deposition	Cu_2O
Co	0.1 M $CoSO_4.6H_2O$ 0.1 M NaOAc 0.1 M Na_2SO_4	7.52	Constant potential at 1.0 V; anodic deposition	Hydrous CoO_x ($x < 2$)
Fe	0.1 M $Fe(NH_4)_2(SO_4)_2 \cdot 6H_2O$ 0.2 M NaOAc 0.1 M Na_2SO_4 (nitrogen saturated)	6.80	Constant potential at -0.1 V; anodic deposition	Hydrous FeO_x ($x < 1.5$)
Mn	0.1 M $Mn(OAc)_2.4H_2O$ 0.1 M Na_2SO_4	7.50	Constant potential at +0.4 V; anodic deposition	Hydrous MnO_x ($x < 2$)

where Ac = acetate.

Under illumination, electrodeposited copper oxide films exhibit p-type semiconducting behavior. The electrolyte used to demonstrate this effect was the acetonitrile-phthalonitrile ($o\text{-}C_6H_4(CN)_2$) system utilized with p-type Cu_2O by Bard, et al [9]. Figure 4 shows the current-potential characteristics of the

film-covered electrode under illumination with chopped light (tungsten-halogen lamp, 80 mW/cm^2). Note that photocurrents in the 100 μA/cm^2 range were observed - a remarkable result considering the unoptimized nature of these as-formed films. The p-type behavior observed for the electrodeposited material substantiates the assignment of Cu_2O as its structure.

Cobalt oxide films anodically deposited at constant potential under the conditions given in Table I are deep yellow (thinner films exhibit interference colors) and appear to have high electrical conductivity. Black films approaching a nominal thickness of 1 μm can be deposited with no observable decay in the deposition current. Deposits formed at +0.8 V appear to be much less conducting, which suggests that a Co(IV) species may be responsible for the high conductivity of films deposited at more positive potentials [10]. As shown by the voltammograms in Fig. 5, in the presence of ferrocyanide, reversible $Fe(CN)_6^{3-/4-}$ redox waves are superimposed on the voltammetric features corresponding to oxidation/reduction of the cobalt oxide film in alkaline solution. The voltammograms shown are stable, but slow changes are observed for sweeps to more negative potentials.

Iron oxide films anodically deposited at constant potential under the conditions given in Table I are pale yellow and can be grown to a nominal thickness of ~300Å, above which the deposition current decays. On films below this apparent limiting thickness, the ferro-ferricyanide reaction proceeds reversibly, whereas, thicker films appear to be insulating. Stable voltammograms with potential cycling between +0.6 and -0.8 V were obtained for thinner films in 0.1 M NaOH. No photoresponse was observed for electrodeposited iron oxide in any of various electrolytes tested.

Like cobalt oxide, manganese oxide films (orange) anodically deposited under the conditions given in Table I are highly conducting as evidenced by the stable deposition currents at film thicknesses approaching the 1 μm range. Under potential cycling, these films slowly dissolve in acidic or basic electrolytes, but are apparently stable in neutral 0.1 M Na_2SO_4 (pH 7.5) at potentials between +1.0 and 0.0 V. Figure 6 shows voltammograms obtained for manganese

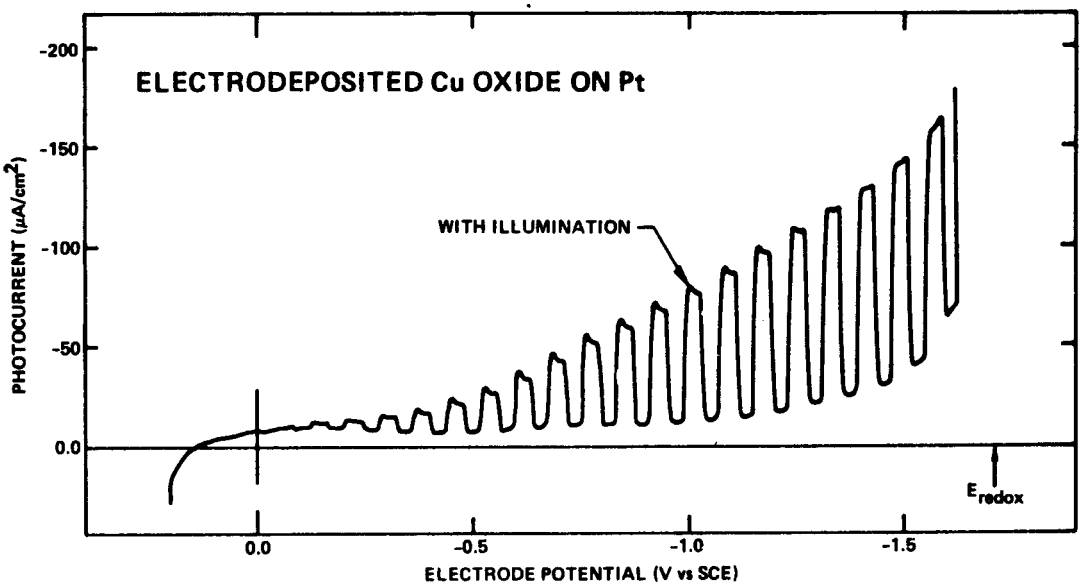

Fig. 4 Voltammetric behavior at 50 mV/sec of a stationary electrodeposited copper oxide film (5000Å) on platinum under illumination with chopped light (80 mW/cm^2) in acetonitrile solution containing 0.1 M phthalonitrile and 0.1 M $NaClO_4$.

oxide films in the latter electrolyte, with and without added ferrocyanide ion. The good conductivity of the film is also evident from the reversible $Fe(CN)_6^{3-/4-}$ redox wave.

In conclusion, thin uniform metal oxide/hydroxide films of copper, nickel, cobalt, iron, and manganese can be electrodeposited onto conducting substrates from acetate-buffered aqueous solutions. The as-formed copper(I) oxide films exhibit p-type photoactivity. In most cases, the other electrodeposited oxides are electrically conducting, especially those of manganese and cobalt. The nickel oxide exhibits electrochromic behavior.

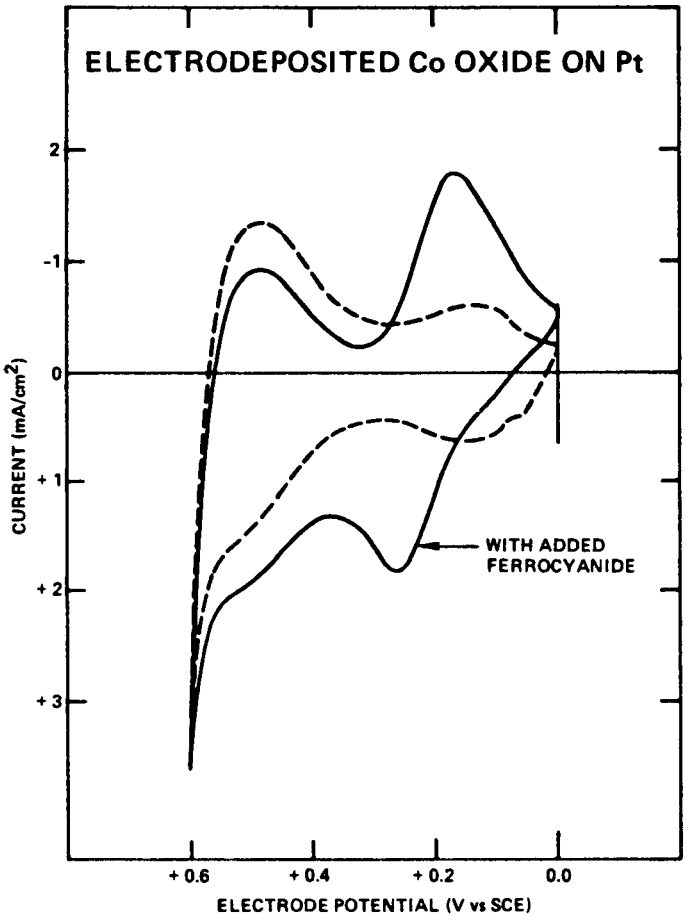

Fig. 5 Cyclic voltammogarms at 50 mV/sec for a stationary electrodeposited cobalt oxide film (600Å) on Pt in 0.1 M NaOH, with (solid curve) and without (dashed curve) added ferrocyanide (0.01 M).

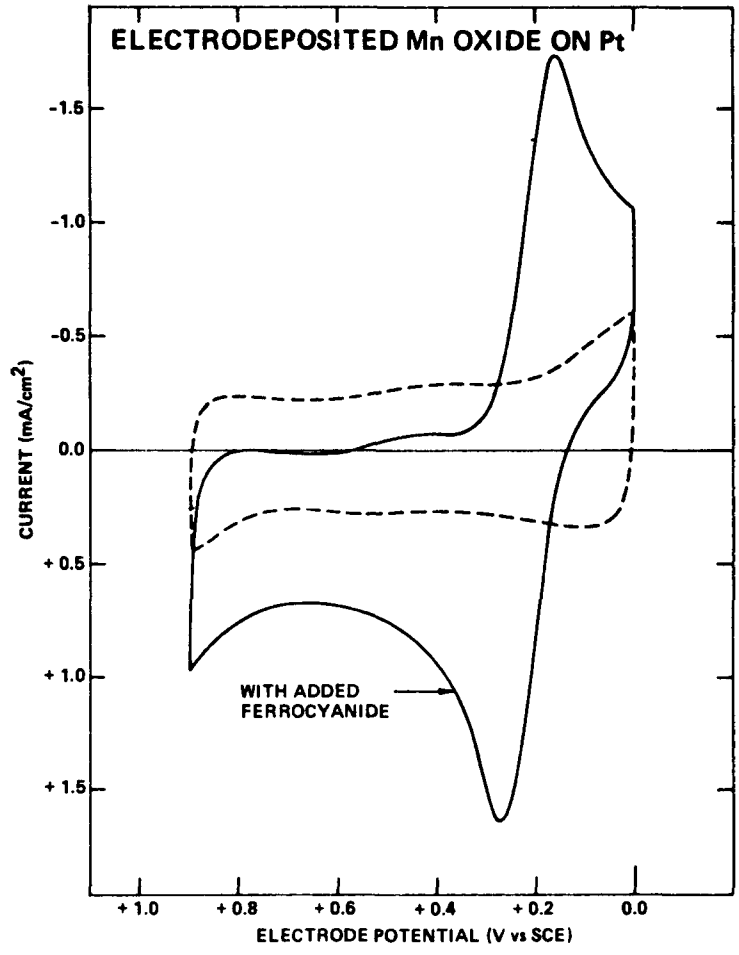

Fig. 6 Cyclic voltammogarms at 50 mV/sec for a stationary electrodeposited manganese oxide film (600Å) on Pt in 0.1 M Na_2SO_4, with (solid curve) and without (dashed curve) added ferrocyanide (0.01 M).

ACKNOWLEDGEMENT

The authors gratefully acknowledge support of this work by the Solar Energy Research Institute under Subcontract No. XG-0-9276.

REFERENCES

1. B. MacDougall and M. J. Graham, J. Electrochem. Soc., 128, 2321 (1981).

2. S. M. Wilhelm and N. Hackerman, J. Electrochem. Soc., 128, 1668 (1981).

3. J. L. Ord, Surface Sci., 56, 413 (1976).

4. L. D. Burke and T. A. M. Twomey, J. Electroanal. Chem., 134, 353 (1982).

5. S. H. Glarum and J. H. Marshal, J. Electrochem. Soc., 129, 535 (1982).

6. C. C. Liang, in "Encyclopedia of Electrochemistry of the Elements", V. 1, A. Bard, ed., Marcel Dekker, New York, 1973, p. 349.

7. E. Barchese, H. C. Chagas, and S. Wolynec, An. Acad. Brasil. Ciênc., 53, 309, (1981).

8. M. Cohen, D. Mitchell, and K. Hashimoto, J. Electrochem. Soc., 126, 442 (1979).

9. G. Nagasubramanian, A. S. Gioda, and A. J. Bard, J. Electrochem. Soc., 128, 2158, (1981).

10. L. D. Burke, M. E. Lyons, and O. J. Murphy, J. Electroanal. Chem., 132, 247, (1982).

APPENDIX IV

Paper on electrodeposition of conducting ruthenium oxide films, to be submitted to the Journal of the Electrochemical Society.

ELECTROCHEMICAL DEPOSITION OF CONDUCTING RUTHENIUM OXIDE FILMS FROM SOLUTION

Dennis P. Anderson and Leslie F. Warren
Rockwell International
Microelectronics Research & Development Center
Thousand Oaks, CA 91360

In the last decade, ruthenium oxide, RuO_x ($x \leq 2$), has been used extensively as the active anode electro-catalyst constituent for Cl_2 and O_2 evolution reactions, in chlorate production, and in metal electrowinning from mixed chloride-sulfate solutions [1-3]. More recently, this material has been incorporated in several light-induced water electrolysis schemes [4-8] and apparently possesses the ability to inhibit CdS photocorrosion by acting as a hole scavenger [6-8]. The numerous applications for this catalyst material certainly warrant further studies of its electrochemical properties on a variety of substrates, e.g., semiconductors. The lack of a simple technique for controlled deposition of ruthenium oxide onto conducting substrates prompted us to investigate an electrochemical approach to this problem. We describe here a new method for electrodepositing conducting ruthenium oxide films from stable aqueous solutions containing a ruthenium(II) complex.

As with manganese oxide, MnO_x [9,10], it was assumed that anodic electrodeposition of RuO_x may take place from an aqueous solution of the corresponding M^{2+} ion. Preparation and isolation of air-sensitive aqua ion $Ru(OH_2)_6^{2+}$ salts is, however, a tedious procedure involving use of expensive and reactive RuO_4 and ion-exchange chromatography procedures [11]. A more accessible ruthenium(II) species which may cleanly oxidize to RuO_x is derived from the very stable organometallic complex $[Ru(\eta^6\text{-}C_6H_6)Cl_2]_2$, formed in virtually quantitative yield from commercial "$RuCl_3 \cdot 3H_2O$" and 1,3- or 1,4-cyclohexadiene [12]. Treatment of an aqueous solution of this species with two equivalents of $AgBF_4$ generated

the yellow aquated $Ru(C_6H_6)(OH_2)_3^{2+}$ species [12a, 13], which appeared to be stable indefinitely over a wide range of pH values. (Although air sensitivity was not apparent, typically the solutions were stored under an inert atmosphere). The effect of the coordinated benzene is to stabilize the ruthenium(II) oxidation state compared with the aqua $Ru(OH_2)_6^{2+}$ ion [11].

The anodic electrodeposition of RuO_x on a rotating Pt disc electrode (400 rpm) took place at a constant potential, +0.9 V (vs SCE), from aqueous solutions containing the $Ru(C_6H_6)(OH_2)_3^{2+}$ complex (0.04 M), adjusted to pH 5; 0.1 M sodium perchlorate was used as supporting electrolyte.

$$[Ru(C_6H_6)Cl_2]_2 \xrightarrow[-AgCl]{Ag^+} Ru(C_6H_6)(OH_2)_3^{2+} \xrightarrow[pH \sim 5]{+0.9\ V} RuO_x + C_6H_6$$

Films of thickness corresponding to 20-30 mC/cm^2 were typically grown, though much thicker films were attainable since the deposits are conducting. Using a cubic approximation of the RuO_2 unit cell as 4.6Å, these charges corresponded to thicknesses of 600-1000Å.

The resulting smooth brown films were conducting in aqueous electrolytes, as perceived from the stable anodic deposition current and from their behavior in the presence of a redox couple. Figure 1, shows the current-potential characteristics of a 600Å film on Pt in a pH 4 buffer (phthalate) electrolyte with and without added $Fe(CN)_6^{4-}$ ion; the voltammetric behavior of the redox couple is essentially unaffected by the presence of the oxide film. Similar behavior was observed with ferrocene in an acetonitrile/0.1 M tetraethylammonium perchlorate electrolyte, however, the voltammetric response of the film itself was greatly suppressed in acetonitrile relative to aqueous electrolytes [14]. These results parallel our findings with electrodeposited MnO_x and other transition metal oxide films [10].

The reversible nature of the electrodeposited ruthenium oxide was further demonstrated by its behavior in 0.1 M perchloric acid shown in Figure 2, where at any potential in the sweep, an almost reversible behavior was observed as the sweep direction was changed. This was

manifested as a rapid current change from anodic to cathodic at a magnitude nearly the same as that on the immediately previous anodic sweep; the effect is most pronounced in low pH media. Although the current-potential profiles for our electrodeposited films differed somewhat from those of the reversible films generated by anodic/cathodic potential cycling on ruthenium metal [15], the overall electrochemical properties were similar. The reversible behavior of these films has been attributed to a mixed valency Ru(III-IV) oxide/hydroxide in which a rapid redox process (involving protonation) can occur with kinetic facility [15], i.e., formally, $RuO_2+H^++e^- \rightleftharpoons RuO(OH)$.

Slow dissolution of the fresh electrodeposited ruthenium oxide films occurred during potential cycling in aqueous electrolytes. In the pH 4 buffer solution, the films remained intact provided cycling was limited to the range from +0.6 to -0.2 V [16]. At more positive potentials in the anodic sweep, an anodic current resulted which was apparently due to both dissolution, involving soluble higher oxidation states, and water oxidation; at high pH's (>10), dissolution predominated and orange RuO_4^{2-} streamed off the electrode surface. In acidic electrolytes, oxygen evolution was observed at potentials >+0.8 V; polarization curves in 0.5 M H_2SO_4 indicated that the overvoltage for oxygen evolution on the RuO_x films is less by 320 mV than that on Pt [17]. Dissolution was also evident, however, and emphasized the importance of stabilizing ruthenium oxide by combination with TiO_2 or other oxides [1,15,18].

In conclusion, it is possible to electrochemically deposit conducting films of ruthenium oxide from an aqueous solution of the benzene-ruthenium(II)-aqua complex. The films slowly dissolve in aqueous electrolytes upon potential cycling, yet appear to be catalytic with regards to water oxidation. Results of further examinations of these films on a variety of substrates, including semiconductors, will be the subject of a later publication.

Acknowledgements

The authors gratefully acknowledge support of this work by the Department of Energy through contract number XP-9-8002-1 from the Solar Energy Research Institute, Golden, Colorado.

References

1. A. Nitola, Stud. Phys. Theor. Chem., 11 (Electrodes Conduct.), 627 (1981).
2. R. S. Yeo, J. Orehotsky, and S. Srinivasan, J. Electrochem. Soc., 128, 1900 (1981).
3. A. J. Scarpellino, G. L. Fisher, Jr., J. Electrochem. Soc., 129, 515, 522 (1982).
4. E. Amouyal, P. Keller, and A. Moradpour, J. Chem. Soc. Chem. Commun., 1019 (1980).
5. J. Kiwi, E. Borgarello, E. Pelizzetti, M. Visca, and M. Grätzel, Angew. Chem. Int. Ed. Engl., 19, 646 (1980); same authors, Nature, 289, 158 (1981).
6. K. Kalyanasundaram, E. Borgarello, D. Duanghong, and M. Grätzel, Angew. Chem. Int. Ed. Engl., 20, 987 (1981).
7. K. Kalyanasundaram, E. Borgarello, and M. Grätzel, Helv. Chim. Acta., 64, 362 (1981).
8. M. Grätzel, Acc. Chem. Res., 14, 376 (1981), and references therein.
9. E. Barchese, H. C. Chagas, and S. Wolynec, An. Acad. Brasil. Ciêne., 53, 309 (1981) and references therein.
10. L. F. Warren and D. M. Tench, to be submitted for publication.
11. P. Bernhard, H. Lehmann, and A. Ludi, J. Chem. Soc. Chem. Commun., 1216 (1981).
12. (a) R. A. Zelonka and M. C. Baird, Canad. J. Chem., 50, 3063 (1972); (b) M. A. Bennett and A. K. Smith, J. Chem. Soc. Dalton, 233 (1974).
13. R. O. Gould, C. L. Jones, D. R. Robertson, and T. A. Stephenson, J. Chem. Soc. Chem. Comm., 222 (1977).
14. Similar observations were made with other RuO_x electrodes: D. R. Rolison, K. Kuo, M. Umana, D. Brundage, and R. W. Murray, J. Electrochem. Soc., 126, 407 (1979).

15. S. Hadzi-Jordanov, H. Angerstein-Kozlowska, M. Yukovic, and B. E. Conway, J. Electrochem. Soc., 125, 1471 (1978); M. Yukovic, H. Angerstein-Kozlowska, and B. E. Conway, J. Appl. Electrochem., 12, 193 (1982).

16. The theoretical domain of passivation of ruthenium, corresponding to the formation of $RuO_2 \cdot 2H_2O$ and $Ru(OH)_3$, is limited to a 600 mV range at pH 4 according to M. Pourbaix, Atlas of Electrochemical Equilibria in Aqueous Solutions, NACE, Houston, TX, 1974.

17. Compare with the results of C. Iwakura, K. Hirao, and H. Tamura, Electrochim. Acta., 22, 329, 335 (1977).

18. A. Mills and M. L. Zeeman, J. Chem. Soc. Chem. Comm., 948 (1981).

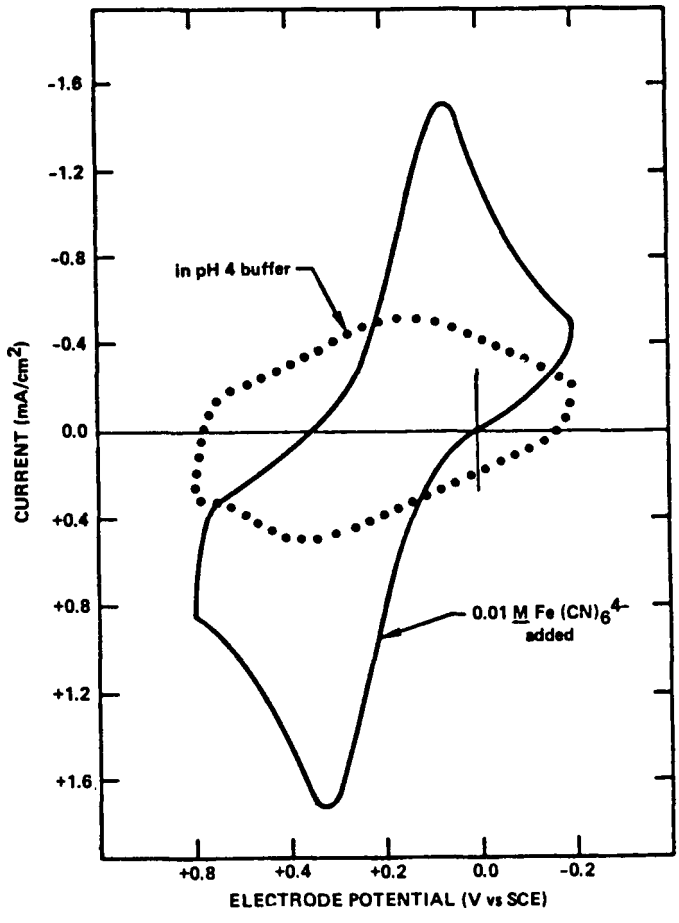

Figure 1. Cyclic voltammograms at 50 mV/sec for an electrodeposited ruthenium oxide film (600Å) on Pt in a pH 4 buffer (phthalate), with solid curve) and without (dotted curve) added ferrocyanide (0.01 M)..

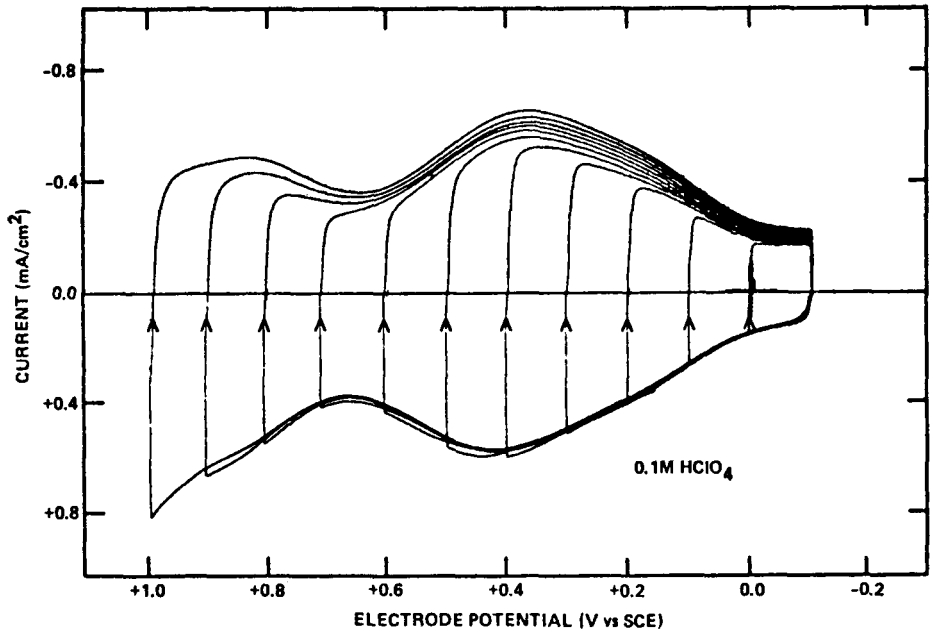

Figure 2. Cyclic voltammograms of an electrodeposited ruthenium oxide film (1000Å) on Pt in 0.1 M $HClO_4$; the potential sweep direction was changed (designated by arrows) from anodic to cathodic at increasing 100 mV intervals; sweep rate 50 mV/sec.

APPENDIX V

Paper on electrochemical photocapacitance spectroscopy published in the Journal of the Electrochemical Society, 129, 891 (1982).

Reprinted from JOURNAL OF THE ELECTROCHEMICAL SOCIETY
Vol. 129, No. 4, April 1982
Printed in U.S.A.

Electrochemical Photocapacitance Spectroscopy: A New Method for Characterization of Deep Levels in Semiconductors

Ron Haak, Cameron Ogden,* and Dennis Tench*

Rockwell International, Microelectronics Research and Development Center, Thousand Oaks, California 91360

Solid-state photocapacitance spectroscopic techniques have been used by various workers, e.g. (1-3), to characterize deep levels in semiconductor materials, but the analogous electrochemical method, which we call electrochemical photocapacitance spectroscopy (EPS), has received only incidental attention (4). This is unfortunate since EPS is expected to be more sensitive than similar solid-state methods because leakage currents can be considerably reduced in electrochemical systems by adjusting the availability of electronic states in the electrolyte, and the monolayer-sharp junction with transparent solutions permits more light to be focused on the area of interest, i.e., the space charge region. EPS is also relatively simple to perform and, if the electrolyte is chosen properly, non-destructive.

In the EPS method, the capacitance of a reverse-biased semiconductor electrode is measured as a function of the wavelength of incident sub-bandgap light. The electrostatic situation and possible phototransitions for an n-type semiconductor are depicted in Fig. 1. In the dark, all of the negative charge in the electrolyte Helmholtz layer must be compensated by fixed ionized donors, resulting in a space charge layer that extends deep into the semiconductor and a space charge capacitance that is generally small ($< 0.1\ \mu F/cm^2$) compared to the Helmholtz layer capacitance ($\sim 20\ \mu F/cm^2$) at sufficiently positive bias voltages (except at very high charge carrier concentrations). In this case, the impedance of the interfacial region is dominated by the space charge and additional charge introduced by optical population/depopulation of traps or interface states significantly affects the thickness of the space charge layer and is readily detected as a change in capacitance. Transitions from bandgap states (electron traps) to the conduction band introduce additional fixed positive charge into the semiconductor space charge region (or at the interface), reducing the thickness of the space charge layer and increasing the capacitance. Similarly, transitions from the valence band to bandgap states (hole traps) result in a decrease in capacitance. Typical plots of capacitance vs wavelength (for sweeps from low to high light energies) yield a series of plateaux, each corresponding to the ionization/saturation of a given bandgap state. The energy levels involved (relative to the appropriate band edge) and the density of states are determined from the onset energy and magnitude of the capacitance change, respectively. It should also be possible to determine the optical absorption cross section for each trap from the rate of change of the capacitance with time under illumination with light of known intensity covering the appropriate energy range, and the emission rate from the rate of decay of the capacitance after interruption of the illumination. It should be mentioned that

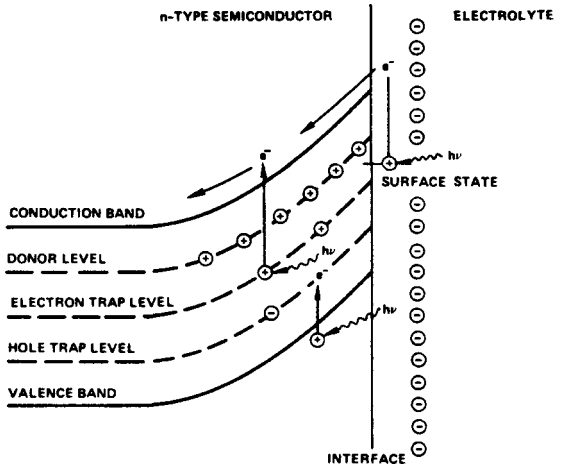

Fig 1 Schematic representation of possible phototransitions for a reverse-biased n-type semiconductor.

*Electrochemical Society Active Members

Key Words: gallium arsenide, traps, electrochemical detection

peaks in the photocapacitance spectrum are obtained for localized transitions involving two bandgap states at the same site (e.g., the ground state and excited state of an impurity) if electrons can be thermally excited from the upper level to the conduction band.

In the present work, EPS measurements were performed automatically with a computerized (Hewlett-Packard Model 9825) apparatus. The real and imaginary components of the electrode impedance were determined by a Solartron Model 1170 Frequency Response Analyzer which automatically averages over many perturbation cycles (50 kcycles for the spectrum reported here). The perturbation voltage was 10 mV (rms). The impedance of the counter electrode (Pt) was eliminated from the measurement by use of a Stonehart Model BC 1200 potentiostat in the three-electrode mode. A Tektronix Model AM501 differential amplifier was employed between the potentiostat and the frequency response analyzer. Monochromatic illumination (1-2 mW/cm^2 having a bandwidth of ~ 8 nm was provided by a 1000 W tungsten-halogen lamp via an Instruments SA Model HT-20 turret monochromator. Measurements were made with increasing light energy (decreasing wavelength). A 1 mm-thick slice of semi-insulating GaAs was used as a filter to minimize interference from bandgap light. A 1.4 μm long-pass filter was used to eliminate second order effects.

The n-GaAs electrode was an undoped <100> single crystal (horizontal Bridgeman-grown), hot-pressed in polychlorotrifluoroethylene plastic so that only the front surface was exposed to the electrolyte. Ohmic contact was provided by AuGe alloy annealed in hydrogen. The charge carrier concentration, determined by Hall measurements, was $4 \times 10^{14}/cm^3$. The surface was finely polished (to 1 μm particle size), and then etched in a 1:1 mixture of H_2SO_4 and 30% H_2O_2 for 10-30 seconds. The cell was Pyrex glass with a quartz window (sealed from the atmosphere and shielded from extraneous light). The electrolyte was argon-saturated acetonitrile containing 0.1 M Et_4NClO_4. The platinum counter electrode was separated from the main cell compartment via a glass frit. The reference electrode was Ag/Ag^+ in acetonitrile (0.1 M $AgNO_3$ + 0.1 M Et_4NClO_4).

Figure 2 shows an EPS spectrum for n-GaAs biased 0.5 V positive of the flatband potential (-0.7 V) in acetonitrile solution at room temperature (22°C). Note that actual data points are given. The excellent sensitivity of the method is evident. The

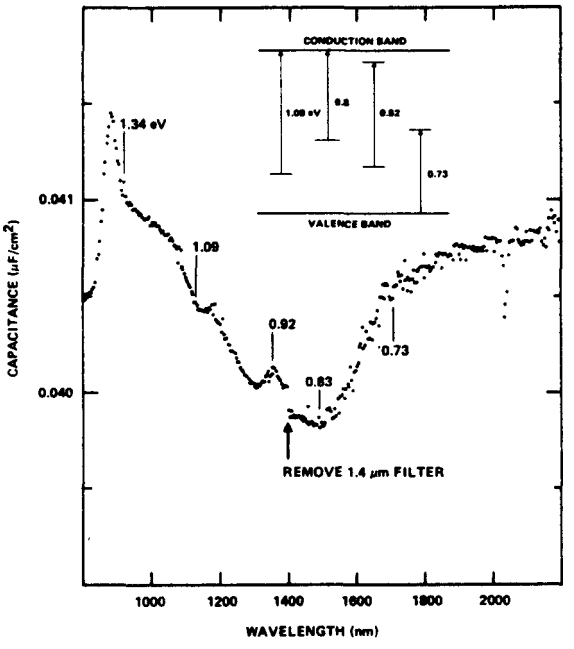

Fig. 2 EPS spectrum (measured at 5 kHz) and associated energy levels/phototransitions for n-GaAs in acetonitrile.

decrease in capacitance at 0.73 eV corresponds to a transition from the valence band to a bandgap state, which reduces the positive charge in the space charge layer (increasing its thickness). This state is apparently the well-known "B" level (5,6) which is neutral when empty and negatively-charged when occupied (7) and has been observed by various solid-state methods, e.g., transient capacitance measurements (7,8), photocapacitance (1-3), deep level transient spectroscopy (5,9), and double source differentiated photocapacitance (10). The "B" level is generally detected in material grown by the horizontal Bridgeman technique or liquid phase epitaxy (LPE), but not in that grown by vapor phase epitaxy (VPE). The density of states calculated here from the change in capacitance, assuming trap saturation and a uniform distribution throughout the space charge layer, is $1 \times 10^{14}/cm^3$, in excellent agreement with the value reported by Lang (9) ($1.4 \times 10^{14}/cm^3$) for similar material.

The peak at 0.92 eV in Fig. 2 is most probably due to chromium, which was found to be present at a concentration of $2 \times 10^{14}/cm^3$ by secondary ion mass spectroscopy (SIMS) and has been shown to introduce a peak at ~ 0.9 eV in solid-state photocapacitance (3,10-12), photoconductivity (13), and optical absorption (14,15) spectra. Kolchanova et al. (13) showed that a

localized transition must be involved, and Lin and Bube (11) suggested that electrons are excited from the ground state to the excited state, $Cr^{2+}(d^4)$, and are then thermally excited to the conduction band. This would explain the observation of a peak instead of a plateau in the spectra. Note that the apparent discontinuity at about 1400 nm in Fig. 2 is associated with removal of the 1.4 μm long-pass filter.

The two capacitance increases/plateaux at higher energies are associated with transitions from bandgap states to the conduction band, which result in increases in positive charge in the space charge region. The first of these transitions, associated with an increase in capacitance at 0.83 eV, could be complementary to the 0.73 eV transition, i.e., involve population/depopulation of the same trap. In this case, 0.83 eV would represent the point at which net depopulation of the trap begins to occur as the rate of excitation of electrons from the trap to the conduction band exceeds the transition rate of electrons from the valence band to the trap. On the other hand, a separate trap, involving a transition whose onset at about 0.8 eV is obscured by the occurrence of the chromium and 0.73 eV transitions, may be involved. In any case, this transition probably corresponds to the well-known EL2 state (16,17) which is the dominant trap in bulk and VPE material and is generally given as ~ 0.8 eV (16). The origin of EL2 is unclear. The second transition (onset at 1.09 eV) is less frequently observed but may involve EL2 and the X conduction band minimum (18,19), or a gallium-impurity donor complex (20). Calculated values for the densities of both of these states ~ $10^{14}/cm^3$, which appear reasonable when compared with the various literature results.

Note that the increase in capacitance at 1.34 eV must correspond to the onset of interband transitions since it is observed for both n- and p-type material. Such "bandgap" light may pass through the GaAs filter because of band tailing differences between the filter and the crystal under study, or could correspond to relatively weak transitions. The capacitance decrease above 900 nm results from the increased effectiveness of the GaAs filter in removing higher-energy bandgap light.

In summary, the results presented here show that electrochemical photocapacitance spectroscopy (EPS) is an extremely sensitive means for characterization of deep levels in semiconductor materials. For horizontal Bridgeman-grown n-GaAs, a hole trap (0.73 eV above the valence band edge), the chromium phototransition (peak at 0.92 eV), and two electron traps (~0.8 and 1.09 eV below the conduction band edge) were detected. The energies and densities of states for these levels correspond well with values reported in the literature for solid-state studies of similar material. Comparable success has also been attained for characterization of n-CdSe by EPS (21).

ACKNOWLEDGEMENT

This work was supported in part by the Solar Energy Research Institute under contract number XG-0-9276.

REFERENCES

1. F. D. Hughes, Acta Electonica, 15, 43 (1972).
2. K. Sakai and T. Ikoma, Appl. Phys., 5, 165 (1974).
3. D. Bois, J. Physique, 35, C3-241 (1974).
4. D. M. Tench and H. Gerischer, J. Electrochem. Soc., 124, 1612 (1977).
5. D. V. Lang and R. A. Logan, J. Appl. Phys., 47, 1533 (1976).
6. A. Mitonneau, G. M. Martin and A. Mircea, Electronics Lett., 13, 666 (1977).
7. R. Williams, J. Appl. Phys., 37, 3411 (1966)
8. T. Ikoma and B. Jeppsson, Proc. Int. Sym. GaAs and Related Compounds, Inst. of Phys., 75 (1972).
9. D. V. Lang, J. Appl. Phys., 45, 3023 (1974).
10. A. M. White, P. Porteous and P. J. Dean, J. Electronic Mat., 5, 91 (1976).
11. A. L. Lin and R. H. Bube, J. Appl. Phys., 47, 1859 (1976).
12. P. K. Vasudev and R. H. Bube, Solid-State Electronics, 21, 1095 (1978).
13. N. M. Kolchanova, D. N. Nasledov, M. A. Mirdzhalilova and V. Yu. Ibragimov, Soviet Phys.-Semicond., 4, 294 (1970).
14. G. A. Allen, Brit. J. Appl. Phys., 2-1, 593 (1968).
15. D. Bois and P. Pinard, Phys. Rev. B, 9, 4171 (1974).
16. A. Ashby, G. G. Roberts, D. J. Ashen and J. B. Mullin, Solid-State Commun., 20, 61 (1976).
17. G. M. Martin, A. Mitonneau and A. Mircea, Electronics Lett., 13, 191 (1977).
18. G. M. Martin, Appl. Phys. Lett., 39, 747 (1981).
19. D. Bois and A. Chantre, Rev. Phys. Appl. F., 15, 631 (1980).
20. E. Farbe, C. R. Acad. Sc. Paris, Ser. B, 270, 848 (1970).
21. R. Haak, C. Ogden and D. Tench, to be published, Proc. ECS Sym. on "Measurement Techniques for Photoelectrochemical Solar Cells," Denver, CO, Oct. 11-16, 1981.

Manuscript submitted Dec. 7, 1981; revised manuscript received ca. Feb. 1, 1982.

Publication costs of this article were assist by Rockwell International.